



## Designed, synthesized and biological evaluation of proteolysis targeting chimeras (PROTACs) as AR degraders for prostate cancer treatment

Jian-Jia Liang<sup>d,1</sup>, Hang Xie<sup>e,1</sup>, Rui-Hua Yang<sup>a,b,c</sup>, Ni Wang<sup>a,b,c</sup>, Zi-Jun Zheng<sup>a,b,c</sup>,  
Chen Zhou<sup>a,b,c</sup>, Ya-Lei Wang<sup>a,b,c</sup>, Zhi-Jia Wang<sup>a,b,c</sup>, Hong-Min Liu<sup>a,b,c,\*</sup>, Li-Hong Shan<sup>a,b,c,\*</sup>,  
Yu Ke<sup>a,b,c,\*</sup>

<sup>a</sup> School of Pharmaceutical Sciences, Zhengzhou University, Zhengzhou, Henan 450001, PR China

<sup>b</sup> Collaborative Innovation Center of New Drug Research and Safety Evaluation, Henan Province, Zhengzhou 450001, PR China

<sup>c</sup> Key Laboratory of Advanced Drug Preparation Technologies, Ministry of Education of China, PR China

<sup>d</sup> School of Pharmacy, Wuhan University, Wuhan, Hubei 430072, PR China

<sup>e</sup> School of Pharmacy, Fudan University, Shanghai 201203, PR China

### ARTICLE INFO

#### Keywords:

Androgen receptor  
PROTAC  
Phthalimide  
Degrons  
Prostate cancer

### ABSTRACT

As a continuation of our research on developing potent and potentially safe androgen receptor (AR) degrader, a series of novel proteolysis targeting chimeras (PROTACs) containing the phthalimide degrons with different linker were designed, synthesized and evaluated for their AR degradation activity against LNCaP (AR+) cell line. Most of the synthesized compounds displayed moderate to satisfactory AR binding affinity and might lead to antagonist activity against AR. Among them, compound **A16** exhibited the best AR binding affinity (85%) and degradation activity against AR. Due to the strong fluorescence properties of pomalidomide derivatives, **B10** was found to be effectively internalized and visualized in LNCaP (AR+) cells than PC-3 (AR-) cells. Moreover, the molecular docking of **A16** with AR and the active site of DDB1-CRBN E3 ubiquitin ligase complex provides guidance to design new PROTAC degrons targeting AR for prostate cancer therapy. These results represent a step toward the development of novel and improved AR PROTACs.

### 1. Introduction

Prostate cancer (PCa) is the second most frequently diagnosed cancer, after lung cancer, in men worldwide<sup>1</sup>. The activation of the androgen receptor (AR) signaling is crucial for PCa development and androgen-independent growth<sup>2,3</sup>. As such, androgen deprivation therapy (ADT), via either surgical or chemical castration, has been the mainstay of treatment for advanced PCa for decades<sup>4,5</sup>. At present, nonsteroidal AR antagonists such as nilutamide, flutamide, and bicalutamide are the most commonly prescribed ADT drugs whose mechanism of action consists of competitively inhibiting androgen-AR binding. However eventually metastatic castration-resistant prostate cancer (CRPC) occurs approximately 18–24 months after the start of therapy, and no cure is currently available<sup>6,7</sup>. Although the mechanisms responsible for the progression of PCa to CRPC are not well-known, it has become clear that AR is often overexpressed in CRPC cells and

promotes their androgen dependent proliferation<sup>8</sup>. Consequently, downregulation of the AR level is regarded as a promising strategy to treat CRPC<sup>9,10</sup>.

Inducing protein degradation by small molecules has recently become a hot spot for drug discovery. Unlike mRNA degradation with siRNA, this technology is best exemplified by Proteolysis Targeting Chimeras (PROTACs), which exploit the unique characteristics of the ubiquitin proteasome system in eukaryotic cells<sup>11</sup>. PROTAC is a heterobifunctional molecule composed of a ligand for the protein of interest, a recognition motif for an E3 ubiquitin ligase and two different ligands connected by a linker<sup>12–16</sup>. To date, several PROTAC molecules targeting AR have been reported (Fig 1). In 2008, Crews *et al* developed the first entirely small-molecule AR PROTAC employed the known Mdm2 ligand nutlin-3a as an E3 ligase recruiting moiety<sup>17</sup>. This complex induced AR degradation was observed at a concentration of 10  $\mu$ M in cells. Another small-molecule based PROTAC approach for targeted AR degradation,

\* Corresponding authors at: Zhengzhou University, Zhengzhou 450001, PR China.

E-mail addresses: [liuhm@zzu.edu.cn](mailto:liuhm@zzu.edu.cn) (H.-M. Liu), [shlh@zzu.edu.cn](mailto:shlh@zzu.edu.cn) (L.-H. Shan), [ky@zzu.edu.cn](mailto:ky@zzu.edu.cn) (Y. Ke).

<sup>1</sup> These authors contributed equally to this work.

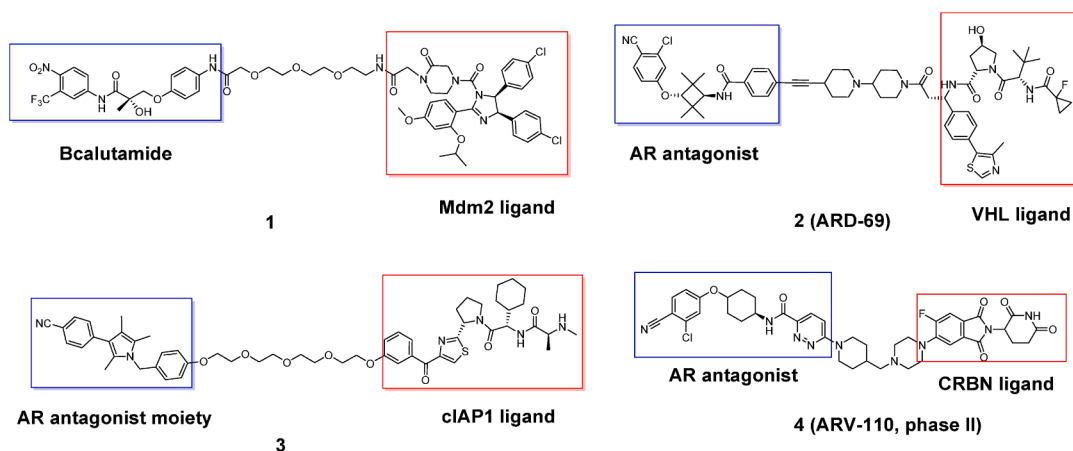


Fig. 1. Structures of representative AR degrader and E3 ligase (red box).

termed cellular inhibitor of apoptosis protein 1 (cIAP1), was reported in 2017 by the Naito group<sup>18</sup>. However, its maximally effective only in the micromolar range and numerous off-target effects were observed, which limit the further development of compound **3**. In 2019, ARD-69 has been recently reported as a new class of small-molecule AR PROTAC degrader, which was designed using several different AR antagonists and a von Hippel-Lindau (VHL) ligand<sup>19</sup>. ARD-69 was shown to be more potent and effective than AR antagonists at inhibiting proliferation and inducing apoptosis of CRPC.

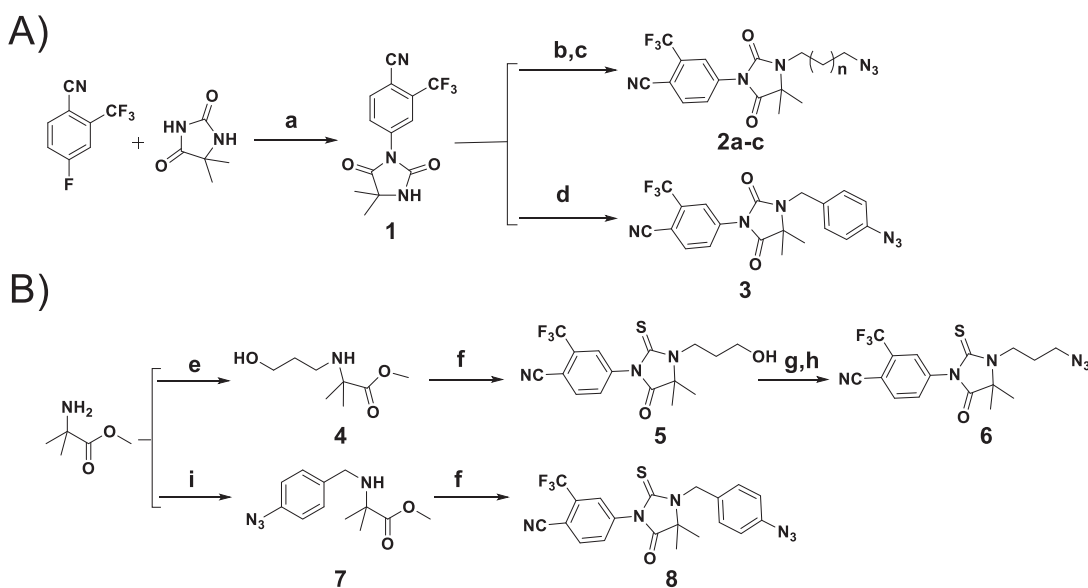
Very recently, cereblon/cullin 4A neddylation degradation systems have been used successfully in the design of PROTAC degraders for different proteins<sup>11,20-26</sup>. The strategy has also been applied to AR PROTAC, such as ARV-110 (Fig 1, 4), which is discovered by Arvinas, and now is being used in the treatment of PCa in the second phase of clinical. Thus, the phthalimide family is often employed as a part of PROTACs to hijack CRBN to target proteins<sup>27</sup>. In this study, we designed and synthesized a series of heterobifunctional compounds based on the high-affinity AR agonist RU59063 derivatives connected through a

1,2,3-triazole linker to a CRBN ligand<sup>28</sup>. Furthermore, we also investigated the effects of length and diversity of linker moieties and other functional group for optimization of these degraders. In addition, we found that pomalidomide can be used as a fluorescent agent to assess the cellular uptake and accumulation of PROTACs.

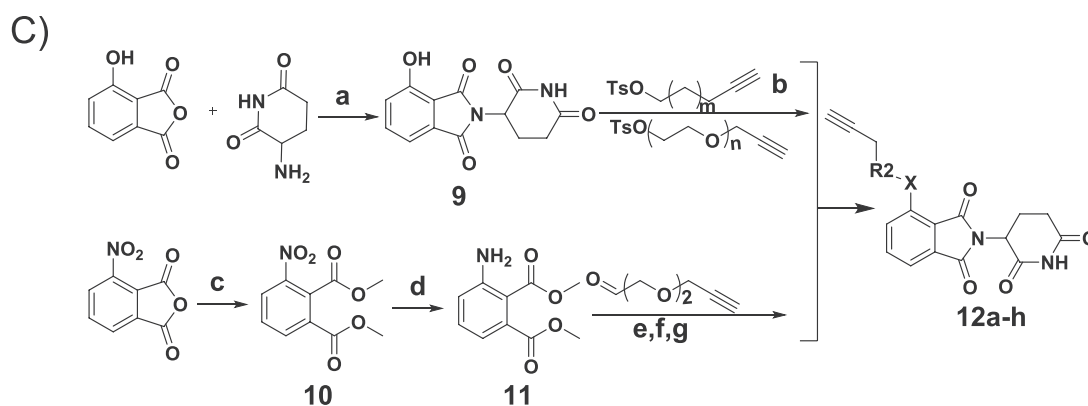
## 2. Result and discussion

### 2.1. Chemistry

The target compounds were obtained through Huisgen 1,3-dipolar cycloaddition of Ru59063 azide derivatives with different phthalimide terminal alkyne moiety. Along with the promising biological activity of 1,2,3-triazole derivatives make them attractive targets in synthetic organic chemistry<sup>29,30</sup>. Compounds **2a-c** and **3** have been reported in our early literature<sup>31,32</sup>. With potassium carbonate as the base, compound **4** and **7** were obtained with a mild yield by reacting the methyl amino acid ester, which were further reacted with 3-fluoro-4-



**Scheme 1.** Synthesis of AR ligands intermediates <sup>a</sup>. <sup>a</sup> Reagents and conditions: (a) K<sub>2</sub>CO<sub>3</sub>, DMF, 45 °C, 5 h; (b) Dibromo alkane, NaH, dry DMF, 0 °C, 2 h; (c) NaN<sub>3</sub>, acetone, 80 °C, 6 h; (d) 1-azido-4-(bromomethyl) benzene, NaH, dry DMF, 0 °C, 1 h. (e, i) Bromo-1-butanol, 1-azido-4-(bromomethyl) benzene, K<sub>2</sub>CO<sub>3</sub>, CH<sub>3</sub>CN, 40 °C, 2–6 h; (f) 3-fluoro-4-methylphenylisothiocyanate, iPOH, triethylamine, rt, 3 h; (g) TsCl, DABCO, CH<sub>2</sub>Cl<sub>2</sub>, 0 °C, 1 h; (h) NaN<sub>3</sub>, acetone, 80 °C, 5 h.



**Scheme 2.** Synthesis of CRBN ligands intermediates <sup>a</sup>. <sup>a</sup> Reagents and conditions: (a) CH<sub>3</sub>COOH, CH<sub>3</sub>COONa, 110 °C. (b) NaHCO<sub>3</sub>, DMF, 80 °C, 5–8 h. (c) 1. CH<sub>3</sub>OH, r.f, 3 h. 2. NaHCO<sub>3</sub>, CH<sub>3</sub>I, DMF, 60 °C, 3 h, 90%. (d) Pd/C, H<sub>2</sub>, Actone, 95%. (e) CH<sub>3</sub>COOH, DCM, Sodium triacetoxyborohydride. (f) NaOH, THF, MeOH, r.f. (g) 2,3-amino piperidine-2, 6-dione, pyridine, 110 °C, 15 h, 55%.

methylphenylisothiocyanate to afford **5** and **8** with good yield. Moreover, the compound **5** was treated with *p*-TsCl and NaN<sub>3</sub> to yield **6** (Scheme 1A and B).

Thalimide intermediates **12a-h** were synthesized as shown in scheme 2. The commercially available 4-hydroxyphthalic anhydride mixed with 3-amino-piperidine-2,6-dione catalyzed by sodium acetate in acetic acid at 110 °C to provide **9**, and then reacted with propargyl-tosylates containing varying aliphatic alcohol or ethylene glycol units afforded the requisite library of cereblon ligase ligands (**12a-g**). Besides, a pomalidomide derivative (**12h**) containing diethylene glycol unit was prepared, 4-nitrophthalic anhydride was treated with the methyl alcohol to generate **10**. Then, the intermediate **11** was obtained by the reduction of **10** in 10% Pd/C. Finally, the key intermediate **12h** was gained through the reaction of **11** with 2-(prop-2-ynyloxy) acetaldehyde in the presence of sodium triacetoxyborohydride and following treatment with 3-amino-piperidine-2,6-dione.

With both azide and alkyne components in hand, we then mixed them to typical conditions for a click reaction (Scheme 3). This involved CuSO<sub>4</sub>/sodium ascorbate as catalyst, and THF/H<sub>2</sub>O to aid in solubilizing the copper catalyst. The reactions were typically very clean and often went to completion within 6 h, and all of the compounds gave moderate to good yields.

## 2.2. Biological evaluation

### 2.2.1. AR binding affinity

In order to evaluate the AR binding affinity of these new PROTAC derivatives, the fluorescence polarization (FP) based binding assay by competition with the fluorescent tracer was carried out, and the results were shown in Figure 2. The affinities are presented as the relative binding affinity (RBA) values, with the binding affinity of testosterone being set at 100%.

In general, most of the synthesized PROTACs showed good RBA affinity values and compound **A16** (85%) displayed the highest AR affinity among the whole series. More interestingly, the binding affinity values were closely related to the length of the R<sub>2</sub> groups, too long or too short chains reduced the binding affinity of the compounds (**A1-18**). Compounds **B1-10** (red bars, Figure 2) with phenyl group showed modest activity except for **B6** (22%) that with a lowest AR affinity. It is worth noting that a sulfur atom on the W substituent dramatically improved compound activity (**A15-18**). Moreover, a decreased efficacy was observed when the propylene glycol moiety of derivative **A11** was extended to tetraethylene glycol (**A14**). Furthermore, changing the R<sub>2</sub> alkyl substituent (**A1-4**) to PEG unit (**A7-A14**) led to a weak decrease of the affinity, which indicated that substituents on the thalidomide ligand moiety might have little impact on determining its binding affinity.

Overall, it was determined that all compounds possessed potent binding affinity and might display antagonist activity against AR.

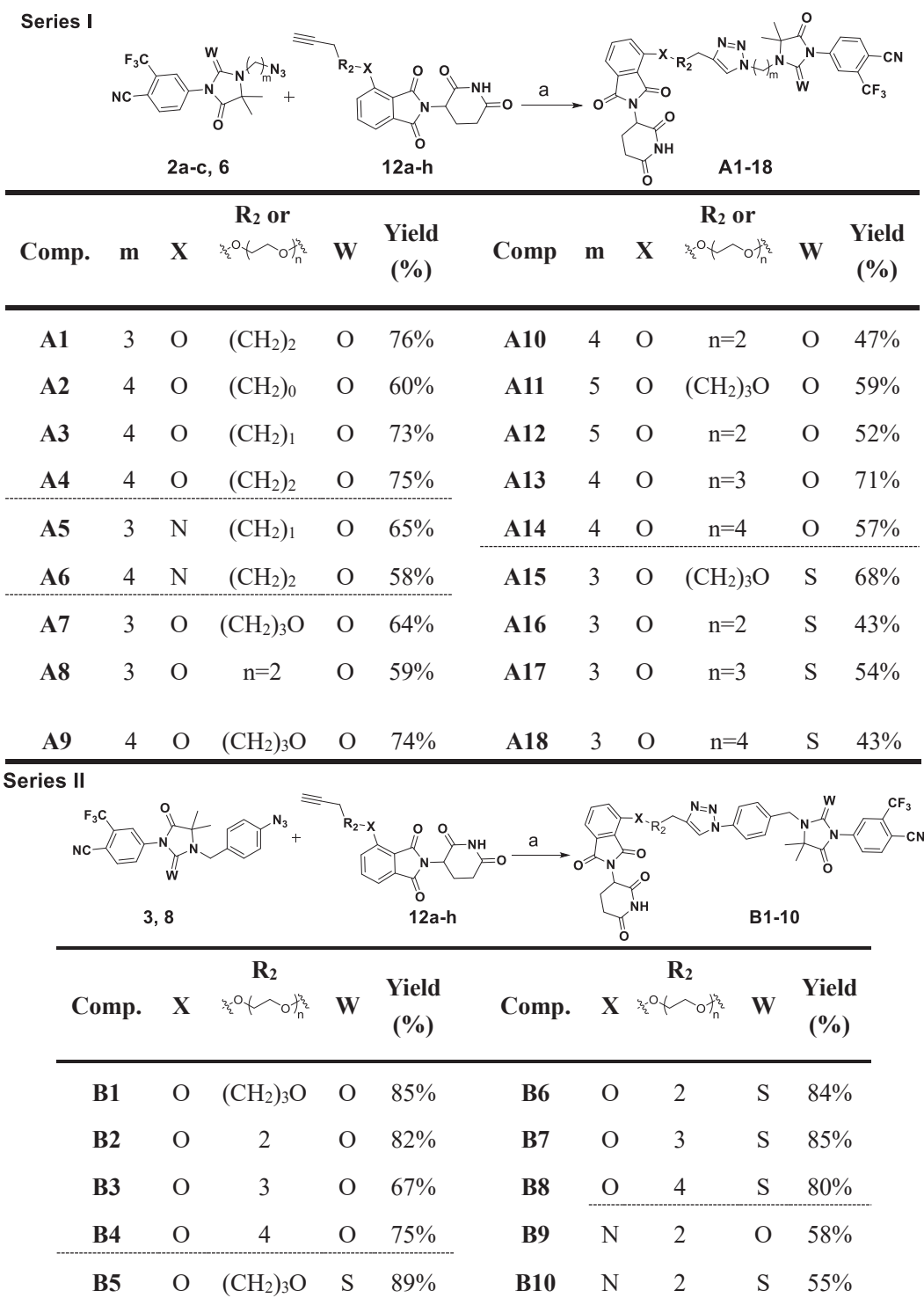
Entry	Cmpd.	affinity % <sup>a</sup> (10 μM)	Entry	Cmpd.	affinity % <sup>a</sup> (10 μM)
1	A1	74.12	16	A16	85.33
2	A2	51.40	17	A17	76.46
3	A3	29.32	18	A18	72.19
4	A4	61.42	19	B1	53.22
5	A5	68.61	20	B2	42.17
6	A6	56.35	21	B3	48.64
7	A7	72.92	22	B4	56.38
8	A8	50.47	23	B5	39.21
9	A9	52.10	24	B6	22.97
10	A10	47.26	25	B7	53.41
11	A11	73.41	26	B8	41.84
12	A12	57.25	27	B9	57.37
13	A13	45.78	28	B10	61.47
14	A14	36.30	29	Enza.	89.15
15	A15	74.53			

### 2.2.2. Confocal microscopy

Due to the strong fluorescence properties of Pomalidomide derivatives (**A5-6**, **B9-10**). We employed LNCaP (AR+) and PC-3 (AR-) for cell imaging to demonstrate the potential of PROTACs as targeted theranostic in cells and the fluorescence response by laser scanning confocal microscopy. As shown in Figure S1, PC-3 (AR-) cells treated with **B10** showed weak fluorescence. Instead, LNCaP (AR+) cells exhibited strong fluorescence intensity upon incubation with **B10** for 24 h, confirming the remarkable cellular uptake of **B10** by LNCaP cells (Figure 3). On the other hand, the cells showed faint fluorescence under the same treatment with pomalidomide. As the stronger fluorescence often means higher cellular uptake, we could deem that the AR targeted ligand could significantly increase the uptake of **B10** in AR overexpressed LNCaP cells and the complex could apply for cell imaging.

### 2.2.3. AR degradation assay

The AR degradation assay of the synthesized PROTACs has been further explored. Considering the AR RBA of this series of compounds, we used 20 μM of some high RBA compounds to test the AR level. The Western blot results of new PROTACs have been presented in Figure S2. Among them, compound **A16** showed equal or better degradation activity compared to other compounds. However, all selected compounds have only a modest effect in reducing the level of AR protein, with the AR degradations ranging from 6% to 32%, respectively (Fig S2), which indicated that these hybrids were essentially inactive against AR degradation. Lastly, we chose the best compound **A16** of the series at three different concentrations (10, 20, and 30 μM) for 24 h, untreated cells were applied as the control. Figure 4A and B revealed that



**Scheme 3.** Synthesis of PROTAC derivatives **A1-18**, **B1-10**. <sup>a, d</sup> Reagents and conditions: (a) CuSO<sub>4</sub>, Na-ascorbate, THF/H<sub>2</sub>O, rt, 2–10 h.

compound **A16** could dose-dependently down-regulate the AR, and it showed good degradation activity at 30 μM. Taken together, these data suggest that more studies are needed to determine if the cereblon/cullin 4A E3 ligase system can be used for the design of highly potent and effective AR degraders.

#### 2.2.4. Molecule docking

To better illustrate the mechanism of compound **A16** degradation at the molecular level, we performed computer modeling using Molecular Operating Environment (MOE version 2014) software. Firstly, we

estimated the binding effect of compound **A16** to AR (PDB: 2axa). As shown in **Figure 5A**, possessing a similar binding mode to other nonsteroidal AR ligands<sup>33</sup>, compound **A16** could also fit into the binding site by the formation of the key hydrogen bond between the cyano group and Gln711, Arg752, the hydrogen bond lengths were 1.82 Å and 1.72 Å, respectively. Moreover, the thalidomide carbonyl group could form a 1.53 Å hydrogen bond with Met742. By analyzing 2D binding mode (**Figure 5B**), we could see that the polarity of the hybrid core structure is significantly increased. In addition, thalidomide ring of **A16** displayed π-π stacking effect with Trp741.

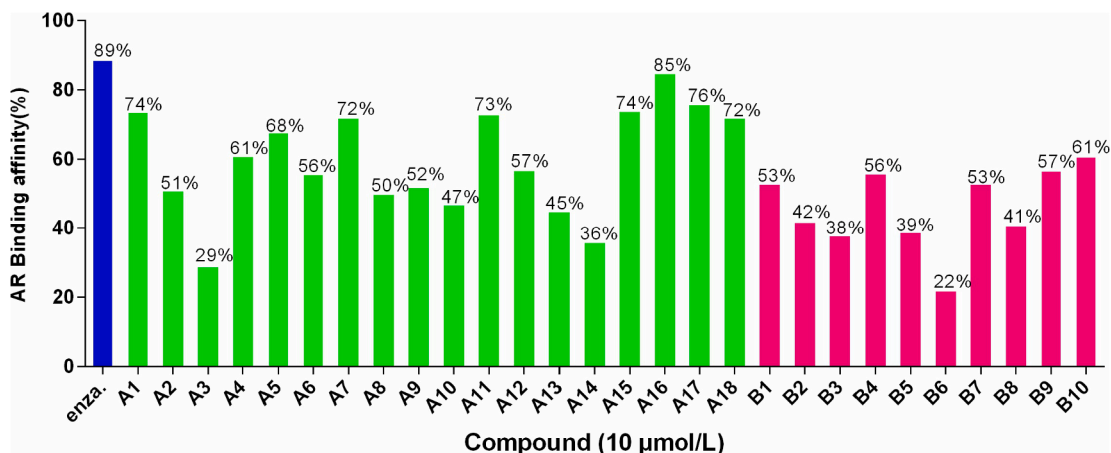


Fig 2. <sup>a</sup> Relative binding affinity (RBA) values are determined by competitive fluorometric binding assays. We set the RBA value of testosterone as 100%.

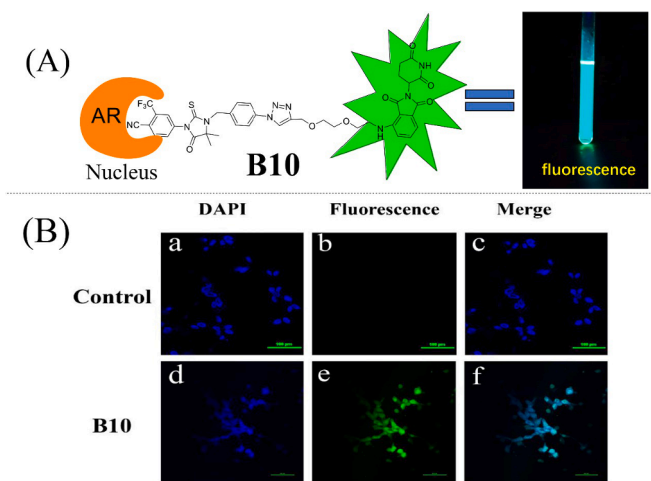


Fig 3. (A) Structure of compound **B10**. (B) Confocal microscopy images of LNCaP cells treated with 10 μM compound **B10** (d – f). Fluorescence from DAPI staining nucleus appears as blue signals (Ex: 340 nm; Em: 450–470 nm) in the left column while fluorescence from **B10** appear as green signals (Ex: 355 nm; Em: 490–520 nm) in the middle column. The right column was the merge of both above. Scale bar: 100 μm.

Then, we verified the binding effect of compound **A16** to DDB1-CRBN E3 ubiquitin ligase (PDB: 4ci3). As shown in Figure 5C and D, we noticed that AR ligand can't fit into the binding site, and mostly exposure to the protein (blue region). In contrast, thalidomide ligand could form hydrogen bonds with Asn353 and Trp402, and the hydrogen

bond length were 2.38 Å and 2.09 Å, respectively. Moreover, piperidine ring of thalidomide displayed  $\pi$ -H stacking effect with Trp382. From these interaction patterns found in the computer modeling, we can provide the basis for the discovery of new and simpler PROTACs.

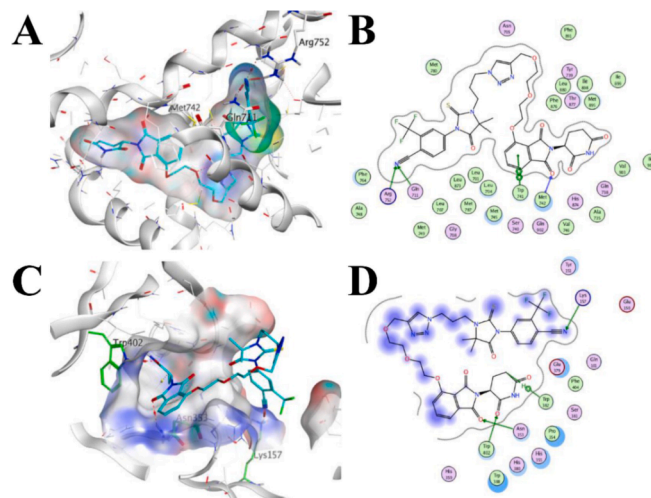


Fig 5. (A) Computer modeling of conjugates **A16** in the active site of AR (PDB: 2axa). (B) 2D complex structures of the AR with **A16**. (C) Docking study of compound **A16** bound to DDB1-CRBN E3 ubiquitin ligase (PDB: 4ci3). (D) 2D complex structures of the CRBN with **A16**, in 2D graph, bright blue region indicates ligand exposure, and hydrogen bonds are shown as green arrow lines.

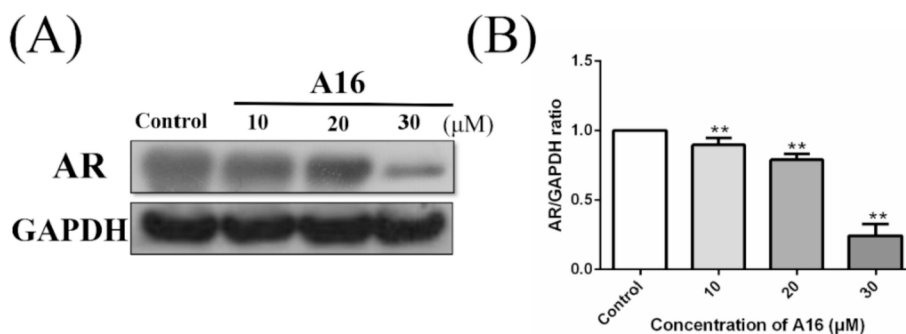


Fig 4. (A) Western blot assay of AR treated with **A16** in different doses from 0 μM to 30 μM. (B) The graph exhibits AR values for **A16**. The whole proteins were extracted, and the AR protein levels were analyzed by Western blotting. (\*)  $P < 0.05$  was considered statistically significant. (\*\*)  $P < 0.01$  was considered statistically highly significant.

### 3. Conclusion

Herein, we have designed, synthesized, and evaluated a type of PROTAC AR degraders using RU59063 derivatives and ligands for cereblon/cullin 4A E3 ligases. We also developed a mild and efficient CuAAC process that allows access to a wide library of new 1,2,3-triazole derivatives with antagonist activity and degradation against the AR. FP competitive experiments showed that most PROTACs displayed satisfactory AR binding affinity and antagonist activity against AR, and compound **A16** (85% VS 89%, Enzalutamide) proved to be the most promising of the series. Additionally, there was greater accumulation of **B10**, in LNCaP (AR+) cells than in PC-3 (AR-) cells. Such differences in accumulation contributed to the selective AR activity *in vivo*. Moreover, the internalization of pomalidomide could be easily visualized by confocal microscopy due to its fluorescence property, hinting at its potential as a targeting theranostic agent. Western blotting assays analyzed the effect of AR degradation and the results showed that PROTAC **A16** have only a modest effect in reducing the level of AR protein in LNCaP cells. Thus, whether the cereblon/cullin 4A E3 ligase system can be used for the design of highly potent and effective AR degraders are needed more studies to determine. Further design and mechanistic studies on these PROTAC conjugates are currently in progress in our group.

### 4. Experimental section

#### 4.1. Materials and methods

Melting points were determined on an X-5 micro-melting apparatus and are uncorrected. Reagents and solvents were purchased from commercial sources and used without further purification. Thin-layer chromatography (TLC) was carried out on glass plates coated with silica gel (Qingdao Haiyang Chemical Co., G60F-254) and visualized by UV light (254 nm). The products were purified by column chromatography over silica gel (Qingdao Haiyang Chemical Co., 200–300 mesh). <sup>1</sup>H NMR and <sup>13</sup>C NMR spectra were recorded on a Bruker 400 MHz and 101 MHz spectrometer, respectively. High resolution mass spectra (HRMS) of all derivatives were recorded on a Waters Micromass Q-T of Micromass spectrometer by electrospray ionization (ESI). The more details of synthesis of intermediate compounds and spectroscopic characterizations were supplied in the [Supporting Information](#).

#### 4.2. Chemistry

##### 4.2.1. General procedures for click reaction (**A1-18** and **B1-10**)

Into a round bottom flask, alkyne derivatives (1.0 equiv) with different side chain lengths (**12a-h**) and appropriate azides (**2a-c**, **3**, **6** and **8**, 1.2 equiv) were dissolved in THF (4 mL), then put 1 mL H<sub>2</sub>O in it, finally, CuSO<sub>4</sub> (1.0 equiv) and Na-ascorbate (3.0 equiv) as catalytic agent to react 2–10 h. Then insoluble matter was filtered and condensed, subsequently, extracted with EtOAc and washed with brine, dried over anhydrous Na<sub>2</sub>SO<sub>4</sub>, filtered, evaporated and the crude product was purified by column chromatography to give products.

##### 4.2.2. Characterization data for final compounds **A1-18** and **B1-10**

**4-(3-(3-(4-(2-((2-(2,6-dioxopiperidin-3-yl)-1,3-dioxoisindolin-4-yl)oxy)ethyl)-1H-1,2,3-triazol-1-yl)propyl)-4,4-dimethyl-2,5-dioxoimidazolidin-1-yl)-2-(trifluoromethyl)benzotrile (**A1**)**. White solid, 76% yield, mp 141–143 °C, <sup>1</sup>H NMR (400 MHz, DMSO-*d*<sub>6</sub>) δ 11.09 (s, 1H), 8.32 (t, *J* = 4.2 Hz, 2H), 8.19 (d, *J* = 1.7 Hz, 1H), 8.04 (dd, *J* = 8.4, 1.8 Hz, 1H), 7.84 (dd, *J* = 8.5, 7.3 Hz, 1H), 7.78–7.69 (m, 1H), 7.50 (dd, *J* = 13.2, 7.5 Hz, 1H), 5.44 (s, 2H), 5.07 (dd, *J* = 12.8, 5.4 Hz, 1H), 4.51 (t, *J* = 7.2 Hz, 3H), 3.47–3.35 (m, 5H), 2.88 (ddd, *J* = 13.9, 5.5 Hz, 1H), 2.56 (s, 2H), 2.25–2.16 (m, 2H), 2.06–1.97 (m, 1H), 1.45 (s, 6H). <sup>13</sup>C NMR (100 MHz, DMSO-*d*<sub>6</sub>) δ 173.71, 172.68, 169.97, 169.74, 168.61, 155.81, 155.78, 142.78, 138.65, 135.83, 134.08, 132.75, 132.32, 131.76, 123.67, 121.27, 120.04, 118.89, 118.26,

116.93, 116.67, 113.05, 64.60, 58.50, 52.77, 48.05, 36.61, 29.68, 24.53, 24.11, 23.91. ESI-HRMS: *m/z* cacl. For C<sub>32</sub>H<sub>27</sub>F<sub>3</sub>N<sub>8</sub>O<sub>7</sub> [M+H]<sup>+</sup>: 693.2033, found 693.2021.

**4-(3-(4-(4-((2-(2,6-dioxopiperidin-3-yl)-1,3-dioxoisindolin-4-yl)oxy)methyl)-1H-1,2,3-triazol-1-yl)butyl)-4,4-dimethyl-2,5-dioxoimidazolidin-1-yl)-2-(trifluoromethyl)benzotrile (**A2**)**. White solid, 60% yield, m.p.:133–135 °C, <sup>1</sup>H NMR (400 MHz, DMSO-*d*<sub>6</sub>) δ 11.10 (s, 1H), 8.31 (d, *J* = 8.4 Hz, 1H), 8.17 (d, *J* = 1.7 Hz, 1H), 8.11 (s, 1H), 8.02 (dd, *J* = 8.4, 1.8 Hz, 1H), 7.81 (dd, *J* = 8.4, 7.4 Hz, 1H), 7.54 (d, *J* = 8.5 Hz, 1H), 7.45 (d, *J* = 7.2 Hz, 1H), 5.07 (dd, *J* = 12.8, 5.4 Hz, 1H), 4.44 (t, *J* = 7.1 Hz, 3H), 3.37 (dd, *J* = 13.6, 6.2 Hz, 2H), 3.16 (t, *J* = 6.4 Hz, 2H), 2.87 (ddd, *J* = 14.2, 5.4 Hz, 1H), 2.25–2.10 (m, 2H), 2.06–2.01 (m, 1H), 1.43 (s, 6H). <sup>13</sup>C NMR (100 MHz, DMSO-*d*<sub>6</sub>) δ 173.71, 172.68, 169.97, 169.74, 168.61, 155.81, 155.71, 151.61, 138.65, 136.92, 133.20, 132.75, 132.32, 131.76, 123.67, 118.92, 118.87, 116.95, 116.93, 116.67, 114.73, 113.05, 68.74, 64.60, 52.77, 48.05, 36.61, 29.68, 27.72, 24.53, 24.11, 23.91. ESI-HRMS: *m/z* cacl. For C<sub>33</sub>H<sub>29</sub>F<sub>3</sub>N<sub>8</sub>O<sub>7</sub> [M+H]<sup>+</sup>: 707.2111, found 707.2120.

**4-(3-(4-(4-(2-((2-(2,6-dioxopiperidin-3-yl)-1,3-dioxoisindolin-4-yl)oxy)ethyl)-1H-1,2,3-triazol-1-yl)butyl)-4,4-dimethyl-2,5-dioxoimidazolidin-1-yl)-2-(trifluoromethyl)benzotrile (**A3**)**. White solid, 73% yield, m.p.:131–133 °C, <sup>1</sup>H NMR (400 MHz, CDCl<sub>3</sub>) δ 8.54 (s, 1H), 8.12 (s, 1H), 7.99 (d, *J* = 8.2 Hz, 1H), 7.92 (d, *J* = 8.4 Hz, 1H), 7.82 (s, 1H), 7.69 (t, *J* = 7.8 Hz, 1H), 7.52–7.44 (m, 2H), 5.45 (s, 2H), 4.96 (dd, *J* = 11.2, 4.8 Hz, 1H), 4.45 (t, *J* = 6.7 Hz, 2H), 3.39 (t, *J* = 7.4 Hz, 2H), 2.94–2.82 (m, 1H), 2.77 (t, *J* = 11.8 Hz, 2H), 2.17–2.05 (m, 1H), 2.07–1.98 (m, 2H), 1.76–1.64 (m, 2H), 1.47 (d, *J* = 12.6 Hz, 6H). <sup>13</sup>C NMR (100 MHz, CDCl<sub>3</sub>) δ 173.71, 172.68, 169.97, 169.74, 168.61, 155.81, 155.78, 142.78, 138.65, 135.83, 134.08, 132.75, 132.32, 131.76, 123.67, 121.27, 120.04, 118.89, 118.26, 116.93, 116.67, 113.05, 64.60, 58.50, 52.77, 51.79, 40.72, 29.68, 27.72, 24.88, 24.53, 24.11. ESI-HRMS: *m/z* cacl. For C<sub>34</sub>H<sub>31</sub>F<sub>3</sub>N<sub>8</sub>O<sub>7</sub> [M+H]<sup>+</sup>: 721.2368, found 721.2359.

**4-(3-(4-(4-(3-((2-(2,6-dioxopiperidin-3-yl)-1,3-dioxoisindolin-4-yl)oxy)propyl)-1H-1,2,3-triazol-1-yl)butyl)-4,4-dimethyl-2,5-dioxoimidazolidin-1-yl)-2-(trifluoromethyl)benzotrile (**A4**)**. White solid, 75% yield, m.p.:154–156 °C, <sup>1</sup>H NMR (400 MHz, CDCl<sub>3</sub>) δ 8.68 (s, 1H), 8.13 (s, 1H), 8.00 (d, *J* = 8.3 Hz, 1H), 7.92 (d, *J* = 8.4 Hz, 1H), 7.67 (t, *J* = 7.9 Hz, 1H), 7.52 (s, 1H), 7.45 (d, *J* = 7.2 Hz, 1H), 7.22 (d, *J* = 8.5 Hz, 1H), 4.96 (dd, *J* = 11.9, 5.2 Hz, 1H), 4.38 (t, *J* = 6.8 Hz, 2H), 4.32–4.16 (m, 2H), 3.37 (t, *J* = 7.3 Hz, 2H), 3.00 (dd, *J* = 13.8, 7.0 Hz, 2H), 2.85 (dd, *J* = 22.0, 9.3 Hz, 2H), 2.76 (t, *J* = 7.4 Hz, 2H), 2.29 (dd, *J* = 12.8, 6.4 Hz, 2H), 2.15 (dd, *J* = 15.7, 7.9 Hz, 1H), 2.01–1.92 (m, 2H), 1.70 (dt, *J* = 14.8, 7.4 Hz, 2H), 1.49 (s, 6H). <sup>13</sup>C NMR (100 MHz, CDCl<sub>3</sub>) δ 173.71, 172.68, 169.97, 169.74, 168.61, 155.81, 155.71, 150.80, 138.65, 136.92, 133.20, 132.75, 132.32, 131.76, 123.67, 120.49, 118.92, 118.87, 116.95, 116.93, 116.67, 113.05, 69.99, 64.60, 52.77, 51.79, 40.72, 29.68, 27.72, 25.79, 24.88, 24.53, 24.11, 23.95. ESI-HRMS: *m/z* cacl. For C<sub>35</sub>H<sub>33</sub>F<sub>3</sub>N<sub>8</sub>O<sub>7</sub> [M+H]<sup>+</sup>: 735.2424, found 735.2421.

**4-(3-(3-(4-(2-((2-(2,6-dioxopiperidin-3-yl)-1,3-dioxoisindolin-4-yl)amino)ethyl)-1H-1,2,3-triazol-1-yl)propyl)-4,4-dimethyl-2,5-dioxoimidazolidin-1-yl)-2-(trifluoromethyl)benzotrile (**A5**)**. Yellow solid, 65% yield, m.p.:158–159 °C, <sup>1</sup>H NMR (400 MHz, DMSO-*d*<sub>6</sub>) δ 8.31 (d, *J* = 8.4 Hz, 1H), 8.19 (d, *J* = 1.6 Hz, 1H), 8.04 (d, *J* = 8.4 Hz, 1H), 7.94 (d, *J* = 32.8 Hz, 1H), 7.47 (dd, *J* = 8.4, 7.1 Hz, 1H), 7.01 (dt, *J* = 7.7, 2.7 Hz, 2H), 6.52 (s, 1H), 5.13 (dd, *J* = 13.0, 5.4, 2.7 Hz, 1H), 4.43 (dd, *J* = 11.6, 7.0 Hz, 2H), 4.00–3.82 (m, 1H), 3.37 (t, *J* = 7.2 Hz, 2H), 3.08–2.87 (m, 1H), 2.77 (dd, *J* = 21.4, 13.5 Hz, 2H), 2.60 (dd, *J* = 16.0, 8.5 Hz, 1H), 2.25–2.10 (m, 2H), 2.04 (dt, *J* = 16.5, 13.1 Hz, 1H), 1.78 (dd, *J* = 14.5, 7.4 Hz, 1H), 1.44 (d, *J* = 3.8 Hz, 6H), 1.37–1.13 (m, 2H). <sup>13</sup>C NMR (100 MHz, DMSO-*d*<sub>6</sub>) δ 174.60, 171.48, 169.54, 168.51, 167.32, 152.72, 146.72, 136.75, 136.01, 135.49, 131.92, 129.99, 124.05, 122.48, 121.74, 115.19, 111.02, 108.43, 61.69, 49.05, 47.03, 36.76, 31.16, 29.64, 27.22, 23.48, 22.34, 21.35. ESI-HRMS: *m/z* cacl. For C<sub>33</sub>H<sub>30</sub>F<sub>3</sub>N<sub>9</sub>O<sub>6</sub> [M+H]<sup>+</sup>: 706.2349, found 706.2322.

**4-(3-(3-(4-(3-((2-(2,6-dioxopiperidin-3-yl)-1,3-dioxoisindolin-4-yl)amino)propyl)-1H-1,2,3-triazol-1-yl)propyl)-4,4-dimethyl-2,5-dioxoimidazolidin-1-yl)-2-(trifluoromethyl)benzotrile (A6).**

Yellow solid, 58% yield, m.p.:192.2–193.8 °C, <sup>1</sup>H NMR (400 MHz, CDCl<sub>3</sub>) δ 8.11 (d, *J* = 13.1 Hz, 1H), 7.99 (d, *J* = 8.4 Hz, 1H), 7.92 (d, *J* = 8.4 Hz, 1H), 7.44 (dd, *J* = 8.2, 7.3 Hz, 1H), 7.17 (dd, *J* = 14.7, 7.5 Hz, 1H), 6.88 (d, *J* = 8.3 Hz, 1H), 5.26 (s, 1H), 4.88 (dd, *J* = 11.8, 5.5 Hz, 1H), 4.46 (t, *J* = 12.1 Hz, 2H), 3.88 (t, *J* = 11.8 Hz, 2H), 3.40 (m, 2H), 2.94 (t, *J* = 12.1 Hz, 1H), 2.82–2.70 (m, 3H), 2.36 (m, 2H), 2.09 (d, *J* = 2.9 Hz, 1H), 1.99 (s, 2H), 1.69 (m, 2H), 1.47 (s, 6H). <sup>13</sup>C NMR (100 MHz, CDCl<sub>3</sub>) δ 174.39, 171.02, 168.90, 167.64, 153.14, 145.65, 136.31, 135.64, 135.32, 132.34, 127.94, 122.98, 121.48, 113.18, 110.84, 108.39, 77.24, 62.07, 49.72, 39.85, 37.69, 32.05, 29.76, 23.34, 22.11. ESI-HRMS: *m/z* caclcd. For C<sub>34</sub>H<sub>33</sub>F<sub>3</sub>N<sub>9</sub>O<sub>6</sub> [M+H]<sup>+</sup>: 720.2506, found 720.2511.

**4-(3-(3-(4-(3-((2-(2,6-dioxopiperidin-3-yl)-1,3-dioxoisindolin-4-yl)oxy)propoxy)methyl)-1H-1,2,3-triazol-1-yl)propyl)-4,4-dimethyl-2,5-dioxoimidazolidin-1-yl)-2-(trifluoromethyl)benzotrile (A7).**

White solid. 64% yield, m.p.:196.4–197.5 °C, <sup>1</sup>H NMR (400 MHz, DMSO-*d*<sub>6</sub>) δ 11.11 (s, 1H), 8.31 (d, *J* = 8.4 Hz, 1H), 8.19 (d, *J* = 1.7 Hz, 1H), 8.13 (s, 1H), 8.04 (dd, *J* = 8.4, 1.8 Hz, 1H), 7.80 (dd, *J* = 8.4, 7.4 Hz, 1H), 7.50 (d, *J* = 8.5 Hz, 1H), 7.44 (d, *J* = 7.2 Hz, 1H), 5.09 (dd, *J* = 12.8, 5.4 Hz, 1H), 4.53 (s, 2H), 4.45 (t, *J* = 7.2 Hz, 2H), 4.26 (t, *J* = 6.2 Hz, 2H), 3.65 (t, *J* = 6.2 Hz, 2H), 3.39 (t, *J* = 7.3 Hz, 2H), 2.97–2.80 (m, 1H), 2.65–2.52 (m, 2H), 2.19 (dd, *J* = 13.7, 6.6 Hz, 2H), 2.08–2.03 (m, 1H), 2.02–2.00 (m, 1H), 1.46 (d, *J* = 5.3 Hz, 6H). <sup>13</sup>C NMR (100 MHz, CDCl<sub>3</sub>) δ 174.32, 171.13, 168.53, 167.01, 165.82, 156.54, 153.38, 136.64, 136.20, 135.39, 133.74, 133.44, 128.07, 123.08, 123.03, 119.11, 117.08, 115.92, 114.98, 108.44, 77.25, 66.45, 66.08, 64.37, 62.12, 49.13, 47.81, 37.62, 31.40, 29.87, 29.20, 23.37, 23.34, 22.64. ESI-HRMS: *m/z* caclcd. For C<sub>35</sub>H<sub>33</sub>F<sub>3</sub>N<sub>8</sub>O<sub>8</sub> [M+H]<sup>+</sup>: 751.2373, found 751.2365.

**4-(3-(3-(4-(3-((2-(2,6-dioxopiperidin-3-yl)-1,3-dioxoisindolin-4-yl)oxy)ethoxy)ethoxy)methyl)-1H-1,2,3-triazol-1-yl)propyl)-4,4-dimethyl-2,5-dioxoimidazolidin-1-yl)-2-(trifluoromethyl)benzotrile (A8).**

White solid. 59% yield, m.p.:206.4–207.9 °C, <sup>1</sup>H NMR (400 MHz, CDCl<sub>3</sub>) δ 8.49 (s, 1H), 8.12 (s, 1H), 7.99 (dd, *J* = 8.4, 1.8 Hz, 1H), 7.93 (d, *J* = 8.5 Hz, 1H), 7.71–7.64 (m, 2H), 7.46 (d, *J* = 7.3 Hz, 1H), 7.27 (d, *J* = 1.7 Hz, 1H), 4.95 (dd, *J* = 12.2, 5.3 Hz, 1H), 4.69 (s, 3H), 4.44 (dd, *J* = 13.4, 6.7 Hz, 2H), 4.38–4.32 (m, 2H), 3.97–3.90 (m, 3H), 3.80 (dd, *J* = 5.5, 2.6 Hz, 3H), 3.76–3.68 (m, 4H), 3.47–3.39 (m, 2H), 2.94–2.81 (m, 2H), 2.79–2.69 (m, 2H), 2.35 (dd, *J* = 13.9, 7.2 Hz, 2H), 2.15–2.07 (m, 1H), 1.91–1.82 (m, 2H), 1.50 (s, 6H). <sup>13</sup>C NMR (100 MHz, DMSO-*d*<sub>6</sub>) δ 174.62, 172.80, 169.90, 166.80, 155.80, 153.16, 145.15, 138.37, 137.05, 136.79, 136.02, 133.10, 130.15, 128.94, 124.22, 121.99, 119.87, 116.14, 115.23, 65.76, 63.21, 62.04, 48.69, 28.75, 22.60, 21.94. ESI-HRMS: *m/z* caclcd. For C<sub>36</sub>H<sub>35</sub>F<sub>3</sub>N<sub>8</sub>O<sub>9</sub> [M+H]<sup>+</sup>: 780.2479, found 780.2469.

**4-(3-(3-(4-(3-((2-(2,6-dioxopiperidin-3-yl)-1,3-dioxoisindolin-4-yl)oxy)propoxy)methyl)-1H-1,2,3-triazol-1-yl)butyl)-4,4-dimethyl-2,5-dioxoimidazolidin-1-yl)-2-(trifluoromethyl)benzotrile (A9).**

White solid. 74% yield, m.p.:186.4–187.9 °C, <sup>1</sup>H NMR (400 MHz, CDCl<sub>3</sub>) δ 8.36 (s, 1H), 8.13 (d, *J* = 1.7 Hz, 1H), 7.99 (dd, *J* = 8.5, 1.9 Hz, 1H), 7.92 (d, *J* = 8.5 Hz, 1H), 7.68 (dd, *J* = 8.4, 7.4 Hz, 1H), 7.57 (s, 1H), 7.46 (d, *J* = 7.3 Hz, 1H), 7.23 (d, *J* = 8.5 Hz, 1H), 4.96 (dd, *J* = 12.2, 5.3 Hz, 1H), 4.65 (s, 2H), 4.39 (t, *J* = 6.9 Hz, 2H), 4.28 (t, *J* = 6.0 Hz, 2H), 3.78 (t, *J* = 5.9 Hz, 2H), 3.41–3.32 (m, 2H), 2.93–2.82 (m, 2H), 2.79 (d, *J* = 10.3 Hz, 2H), 2.34–2.21 (m, 1H), 2.19–2.09 (m, 3H), 2.02–1.94 (m, 2H), 1.71 (t, *J* = 7.6 Hz, 2H), 1.50 (s, 6H), 0.95–0.82 (m, 2H). <sup>13</sup>C NMR (100 MHz, CDCl<sub>3</sub>) δ 175.32, 172.13, 166.53, 162.01, 158.82, 156.54, 151.37, 134.32, 133.27, 132.39, 131.74, 131.44, 127.07, 124.08, 125.03, 118.11, 116.08, 114.92, 112.98, 107.44, 77.25, 66.45, 67.08, 64.38, 62.12, 50.33, 47.81, 37.62, 32.45, 29.63, 29.21, 23.34,

22.65. ESI-HRMS: *m/z* caclcd. For C<sub>36</sub>H<sub>35</sub>F<sub>3</sub>N<sub>8</sub>O<sub>8</sub> [M+H]<sup>+</sup>: 765.2530, found 765.2521.

**4-(3-(4-(4-((2-(2-((2-(2,6-dioxopiperidin-3-yl)-1,3-dioxoisindolin-4-yl)oxy)ethoxy)ethoxy)methyl)-1H-1,2,3-triazol-1-yl)butyl)-4,4-dimethyl-2,5-dioxoimidazolidin-1-yl)-2-(trifluoromethyl)benzotrile (A10).**

White solid. 47% yield, m.p.:197.2–198.6 °C, <sup>1</sup>H NMR (400 MHz, CDCl<sub>3</sub>) δ 8.48 (s, 1H), 8.13 (d, *J* = 1.8 Hz, 1H), 7.99 (dd, *J* = 8.5, 1.9 Hz, 1H), 7.92 (d, *J* = 8.4 Hz, 1H), 7.67 (dd, *J* = 8.4, 7.4 Hz, 1H), 7.59 (s, 1H), 7.46 (d, *J* = 7.2 Hz, 1H), 7.29–7.23 (m, 2H), 4.95 (dd, *J* = 12.1, 5.3 Hz, 1H), 4.67 (s, 2H), 4.40 (t, *J* = 6.9 Hz, 2H), 4.35 (t, *J* = 4.6 Hz, 2H), 3.95–3.90 (m, 2H), 3.80 (dd, *J* = 5.7, 2.8 Hz, 2H), 3.74–3.69 (m, 2H), 3.48 (s, 1H), 3.40–3.33 (m, 2H), 2.85 (dd, *J* = 18.3, 16.0 Hz, 1H), 2.80–2.69 (m, 2H), 2.16–2.08 (m, 1H), 2.02–1.94 (m, 2H), 1.71 (t, *J* = 7.3 Hz, 2H), 1.50 (s, 6H). <sup>13</sup>C NMR (100 MHz, DMSO-*d*<sub>6</sub>) δ 174.62, 172.80, 169.90, 166.80, 155.80, 153.16, 145.15, 138.37, 137.05, 136.79, 136.02, 133.10, 130.15, 128.94, 124.22, 121.99, 119.87, 116.14, 115.23, 65.76, 63.21, 62.04, 48.69, 28.75, 22.60, 21.94. ESI-HRMS: *m/z* caclcd. For C<sub>37</sub>H<sub>37</sub>F<sub>3</sub>N<sub>8</sub>O<sub>9</sub> [M+H]<sup>+</sup>: 795.2636, found 795.2616.

**4-(3-(5-(4-((3-((2-(2,6-dioxopiperidin-3-yl)-1,3-dioxoisindolin-4-yl)oxy)propoxy)methyl)-1H-1,2,3-triazol-1-yl)pentyl)-4,4-dimethyl-2,5-dioxoimidazolidin-1-yl)-2-(trifluoromethyl)benzotrile (A11).**

White solid. 59% yield, m.p.:176.2–177.3 °C, <sup>1</sup>H NMR (400 MHz, CDCl<sub>3</sub>) δ 8.36 (s, 1H), 8.07 (s, 1H), 7.91 (t, *J* = 11.6 Hz, 1H), 7.85 (d, *J* = 8.3 Hz, 1H), 7.65–7.57 (m, 1H), 7.39 (t, *J* = 8.0 Hz, 2H), 7.17 (d, *J* = 8.4 Hz, 1H), 4.88 (dd, *J* = 12.1, 5.1 Hz, 2H), 4.33–4.18 (m, 6H), 3.84–3.59 (m, 4H), 3.28–3.18 (m, 2H), 2.89–2.77 (m, 2H), 2.68 (dd, *J* = 28.5, 13.0 Hz, 2H), 2.20–2.09 (m, 2H), 2.05 (dd, *J* = 17.0, 9.2 Hz, 2H), 1.89 (m, 2H), 1.65 (m, 3H), 1.44 (s, 6H), 1.32 (dd, *J* = 24.7, 11.8 Hz, 2H), 0.83–0.74 (m, 2H). <sup>13</sup>C NMR (100 MHz, CDCl<sub>3</sub>) δ 174.32, 171.13, 168.53, 167.01, 165.82, 156.54, 153.38, 136.64, 136.20, 135.39, 133.74, 133.44, 128.07, 123.08, 123.03, 119.11, 117.08, 115.92, 114.98, 108.44, 77.25, 66.45, 66.08, 64.37, 62.12, 49.13, 47.81, 37.62, 31.40, 29.87, 29.20, 23.37, 23.34, 22.64. ESI-HRMS: *m/z* caclcd. For C<sub>37</sub>H<sub>37</sub>F<sub>3</sub>N<sub>8</sub>O<sub>8</sub> [M+H]<sup>+</sup>: 779.2686, found 779.2682.

**4-(3-(5-(4-((2-(2-((2-(2,6-dioxopiperidin-3-yl)-1,3-dioxoisindolin-4-yl)oxy)ethoxy)ethoxy)methyl)-1H-1,2,3-triazol-1-yl)pentyl)-4,4-dimethyl-2,5-dioxoimidazolidin-1-yl)-2-(trifluoromethyl)benzotrile (A12).**

White solid. 52% yield, m.p.:196.3–197.8 °C, <sup>1</sup>H NMR (400 MHz, CDCl<sub>3</sub>) δ 8.47 (s, 1H), 8.14 (s, 1H), 8.00 (d, *J* = 8.4 Hz, 1H), 7.92 (d, *J* = 8.4 Hz, 1H), 7.27 (s, 4H), 4.95 (dd, *J* = 11.9, 5.1 Hz, 1H), 4.36 (s, 5H), 3.94 (s, 2H), 3.79 (d, *J* = 24.9 Hz, 4H), 3.38–3.28 (m, 2H), 2.93–2.81 (m, 1H), 2.74 (dd, *J* = 22.6, 10.9 Hz, 2H), 2.17–2.07 (m, 1H), 1.97 (s, 2H), 1.73 (s, 2H), 1.51 (s, 6H), 1.38 (s, 2H), 0.93–0.79 (m, 2H). <sup>13</sup>C NMR (100 MHz, CDCl<sub>3</sub>) δ 174.32, 171.13, 168.53, 167.01, 165.82, 156.54, 153.38, 136.64, 136.20, 135.39, 133.74, 133.44, 128.07, 123.08, 123.03, 119.11, 117.08, 115.92, 114.98, 108.44, 77.25, 66.45, 66.08, 64.37, 62.12, 49.13, 47.81, 37.62, 31.40, 29.87, 29.20, 23.37, 23.34, 22.64. ESI-HRMS: *m/z* caclcd. For C<sub>38</sub>H<sub>39</sub>F<sub>3</sub>N<sub>8</sub>O<sub>9</sub> [M+H]<sup>+</sup>: 809.2792, found 809.2791.

**4-(3-(3-(4-((2-(2-((2-(2,6-dioxopiperidin-3-yl)-1,3-dioxoisindolin-4-yl)oxy)ethoxy)ethoxy)methyl)-1H-1,2,3-triazol-1-yl)propyl)-4,4-dimethyl-2,5-dioxoimidazolidin-1-yl)-2-(trifluoromethyl)benzotrile (A13).**

White solid. 71% yield, m.p.:216.3–217.8 °C, <sup>1</sup>H NMR (400 MHz, DMSO-*d*<sub>6</sub>) δ 11.11 (s, 1H), 8.32 (d, *J* = 8.3 Hz, 1H), 8.19 (d, *J* = 1.5 Hz, 1H), 8.12 (s, 1H), 8.04 (d, *J* = 8.3 Hz, 1H), 7.83–7.76 (m, 1H), 7.52 (d, *J* = 8.5 Hz, 1H), 7.45 (d, *J* = 7.2 Hz, 1H), 5.08 (dd, *J* = 12.8, 5.3 Hz, 1H), 4.51 (s, 2H), 4.46 (t, *J* = 7.1 Hz, 2H), 4.36–4.31 (m, 2H), 3.84–3.77 (m, 2H), 3.67–3.61 (m, 2H), 3.52 (d, *J* = 8.3 Hz, 2H), 2.89 (dd, *J* = 22.6, 8.4 Hz, 1H), 2.59 (d, *J* = 18.1 Hz, 2H), 2.17 (dd, *J* = 12.3, 5.0 Hz, 2H), 2.06–1.98 (m, 1H), 1.46 (s, 6H). <sup>13</sup>C NMR (100 MHz, DMSO-*d*<sub>6</sub>) δ 174.62, 172.80, 169.90, 166.80, 155.80, 153.16, 145.15, 138.37, 137.05, 136.79, 136.02, 133.10, 130.15, 128.94, 124.22, 121.99,

119.87, 116.14, 115.23, 65.76, 63.21, 62.04, 48.69, 28.75, 22.60, 21.94. ESI-HRMS:  $m/z$  calcd. For  $C_{38}H_{39}F_3N_8O_{10}$  [M+H]<sup>+</sup>: 825.2741, found 825.2743.

**4-(3-(3-(4-(13-((2-(2,6-dioxopiperidin-3-yl)-1,3-dioxoisindolin-4-yl)oxy)-2,5,8,11-tetraoxatridecyl)-1H-1,2,3-triazol-1-yl)propyl)-4,4-dimethyl-2,5-dioxoimidazolidin-1-yl)-2-(trifluoromethyl)benzonitrile (A14).**

White solid. 57% yield, m.p.:212.6–213.7 °C, <sup>1</sup>H NMR (400 MHz, CDCl<sub>3</sub>) δ 8.78 (s, 1H), 8.12 (d,  $J = 1.6$  Hz, 1H), 7.99 (dd,  $J = 8.4, 1.9$  Hz, 1H), 7.93 (d,  $J = 8.5$  Hz, 1H), 7.72 (s, 1H), 7.67 (dd,  $J = 8.3, 7.5$  Hz, 1H), 7.45 (d,  $J = 7.2$  Hz, 1H), 7.26 (s, 1H), 4.95 (dd,  $J = 12.0, 5.4$  Hz, 1H), 4.68 (s, 2H), 4.46 (t,  $J = 6.7$  Hz, 2H), 4.33 (dd,  $J = 11.7, 6.8$  Hz, 3H), 3.98–3.90 (m, 3H), 3.77 (dd,  $J = 5.6, 3.6$  Hz, 3H), 3.67 (ddd,  $J = 8.6, 5.5, 2.0$  Hz, 13H), 3.48–3.40 (m, 2H), 2.85 (dd,  $J = 10.2, 8.3$  Hz, 1H), 2.80–2.70 (m, 2H), 2.39–2.31 (m, 2H), 2.15–2.07 (m, 1H), 1.50 (s, 6H). <sup>13</sup>C NMR (100 MHz, DMSO-*d*<sub>6</sub>) δ 174.62, 172.80, 169.90, 166.80, 155.80, 153.16, 145.15, 138.37, 137.05, 136.79, 136.02, 133.10, 130.15, 128.94, 124.22, 121.99, 119.87, 116.14, 115.23, 65.76, 63.21, 62.04, 48.69, 28.75, 22.60, 21.94. ESI-HRMS:  $m/z$  calcd. For  $C_{40}H_{43}F_3N_8O_{11}$  [M+H]<sup>+</sup>: 869.3003, found 869.3005.

**4-(3-(3-(4-(3-((2-(2,6-dioxopiperidin-3-yl)-1,3-dioxoisindolin-4-yl)oxy)propoxy)methyl)-1H-1,2,3-triazol-1-yl)propyl)-4,4-dimethyl-5-oxo-2-thioxoimidazolidin-1-yl)-2-(trifluoromethyl)benzonitrile (A15).**

White solid. 68% yield, m.p.:211.4–212.6 °C, <sup>1</sup>H NMR (400 MHz, CDCl<sub>3</sub>) δ 8.25 (s, 1H), 7.95 (t,  $J = 7.1$  Hz, 2H), 7.88 (d,  $J = 1.9$  Hz, 1H), 7.80–7.73 (m, 2H), 7.70–7.63 (m, 3H), 7.45 (d,  $J = 7.2$  Hz, 2H), 7.23 (d,  $J = 8.4$  Hz, 3H), 4.96 (dd,  $J = 12.2, 5.3$  Hz, 2H), 4.66 (d,  $J = 10.6$  Hz, 3H), 4.46 (t,  $J = 6.1$  Hz, 3H), 4.29 (t,  $J = 6.0$  Hz, 4H), 3.78 (dd,  $J = 13.3, 7.2$  Hz, 6H), 2.87 (dd,  $J = 15.8, 13.2$  Hz, 3H), 2.82–2.71 (m, 4H), 2.50 (dd,  $J = 14.7, 7.3$  Hz, 2H), 2.34–2.23 (m, 2H), 2.15 (dd,  $J = 13.0, 7.8$  Hz, 2H), 1.53 (s, 6H). <sup>13</sup>C NMR (100 MHz, CDCl<sub>3</sub>) δ 174.32, 171.13, 168.53, 167.01, 165.82, 156.54, 153.38, 136.64, 136.20, 135.39, 133.74, 133.44, 128.07, 123.08, 123.03, 119.11, 117.08, 115.92, 114.98, 108.44, 77.25, 66.45, 66.08, 64.37, 62.12, 49.13, 47.81, 37.62, 31.40, 29.87, 29.20, 23.37, 23.34, 22.64. ESI-HRMS:  $m/z$  calcd. For  $C_{35}H_{33}F_3N_8O_9S$  [M+H]<sup>+</sup>: 767.2145, found 767.2139.

**4-(3-(3-(4-((2-(2-((2-(2,6-dioxopiperidin-3-yl)-1,3-dioxoisindolin-4-yl)oxy)ethoxy)ethoxy)methyl)-1H-1,2,3-triazol-1-yl)propyl)-4,4-dimethyl-5-oxo-2-thioxoimidazolidin-1-yl)-2-(trifluoromethyl)benzonitrile (A16).**

White solid. 43% yield, m.p.:217.6–218.9 °C, <sup>1</sup>H NMR (400 MHz, CDCl<sub>3</sub>) δ 8.49 (s, 1H), 7.96 (d,  $J = 8.3$  Hz, 1H), 7.88 (s, 1H), 7.76 (d,  $J = 8.3$  Hz, 1H), 7.67 (t,  $J = 7.8$  Hz, 1H), 7.44 (t,  $J = 13.7$  Hz, 1H), 7.26 (s, 2H), 4.96 (d,  $J = 6.9$  Hz, 1H), 4.61 (d,  $J = 79.0$  Hz, 4H), 4.36 (s, 2H), 3.94 (s, 2H), 3.88–3.65 (m, 7H), 2.88 (d,  $J = 16.7$  Hz, 2H), 2.82–2.70 (m, 2H), 2.52 (s, 2H), 2.11 (d,  $J = 5.4$  Hz, 1H), 1.53 (s, 6H). <sup>13</sup>C NMR (100 MHz, CDCl<sub>3</sub>) δ 178.82, 175.03, 171.18, 168.34, 166.96, 165.67, 136.98, 136.58, 135.23, 133.77, 132.12, 127.00, 119.51, 117.32, 116.22, 114.81, 77.26, 71.14, 69.93, 69.40, 65.27, 60.41, 49.16, 41.54, 31.42, 29.70, 28.30, 23.09, 22.64, 21.05, 14.21. ESI-HRMS:  $m/z$  calcd. For  $C_{36}H_{35}F_3N_8O_8S$  [M+H]<sup>+</sup>: 797.2651, found 797.2654.

**4-(3-(3-(4-((2-(2-((2-(2,6-dioxopiperidin-3-yl)-1,3-dioxoisindolin-4-yl)oxy)ethoxy)ethoxy)ethoxy)methyl)-1H-1,2,3-triazol-1-yl)propyl)-4,4-dimethyl-5-oxo-2-thioxoimidazolidin-1-yl)-2-(trifluoromethyl)benzonitrile (A17).**

White solid. 54% yield, m.p.:221.3–222.6 °C, <sup>1</sup>H NMR (400 MHz, CDCl<sub>3</sub>) δ 8.67 (s, 1H), 7.95 (t,  $J = 6.9$  Hz, 1H), 7.88 (d,  $J = 1.5$  Hz, 1H), 7.80–7.73 (m, 1H), 7.67 (dd,  $J = 8.7, 7.1$  Hz, 2H), 7.46 (t,  $J = 6.0$  Hz, 1H), 7.25 (s, 1H), 4.96 (dd,  $J = 11.3, 4.9$  Hz, 1H), 4.70 (s, 2H), 4.47 (t,  $J = 6.6$  Hz, 2H), 4.37–4.31 (m, 3H), 3.94 (dd,  $J = 10.8, 6.0$  Hz, 3H), 3.81–3.75 (m, 5H), 3.74–3.64 (m, 8H), 2.90–2.81 (m, 2H), 2.80–2.70 (m, 2H), 2.55–2.44 (m, 2H), 2.12 (dd,  $J = 7.4, 4.9$  Hz, 2H), 1.53 (s, 6H). <sup>13</sup>C NMR (100 MHz, CDCl<sub>3</sub>) δ 174.32, 171.13, 168.53, 167.01, 165.82, 156.54, 153.38, 136.64, 136.20, 135.39, 133.74, 133.44, 128.07, 123.08, 123.03, 119.11, 117.08, 115.92, 114.98, 108.44, 77.25, 66.45,

66.08, 64.37, 62.12, 49.13, 47.81, 37.62, 31.40, 29.87, 29.20, 23.37, 23.34, 22.64. ESI-HRMS:  $m/z$  calcd. For  $C_{38}H_{39}F_3N_8O_9S$  [M+H]<sup>+</sup>: 841.2513, found 841.2516.

**4-(3-(3-(4-(13-((2-(2,6-dioxopiperidin-3-yl)-1,3-dioxoisindolin-4-yl)oxy)-2,5,8,11-tetraoxatridecyl)-1H-1,2,3-triazol-1-yl)propyl)-4,4-dimethyl-5-oxo-2-thioxoimidazolidin-1-yl)-2-(trifluoromethyl)benzonitrile (A18).**

White solid. 43% yield, m.p.:207.3–208.5 °C, <sup>1</sup>H NMR (400 MHz, CDCl<sub>3</sub>) δ 8.70 (s, 1H), 7.95 (t,  $J = 7.4$  Hz, 1H), 7.89 (s, 1H), 7.77 (dd,  $J = 8.3, 1.7$  Hz, 1H), 7.71–7.63 (m, 2H), 7.45 (d,  $J = 7.3$  Hz, 2H), 7.26 (s, 2H), 4.95 (dd,  $J = 11.7, 5.2$  Hz, 1H), 4.70 (s, 2H), 4.48 (t,  $J = 6.5$  Hz, 2H), 4.35 (dd,  $J = 10.3, 5.8$  Hz, 3H), 3.94 (dd,  $J = 9.2, 4.5$  Hz, 3H), 3.78 (dd,  $J = 8.7, 5.1$  Hz, 5H), 3.68–3.62 (m, 11H), 2.91–2.80 (m, 2H), 2.79–2.72 (m, 3H), 2.54–2.45 (m, 2H), 2.15–2.05 (m, 3H), 1.54 (d,  $J = 6.5$  Hz, 6H). <sup>13</sup>C NMR (100 MHz, CDCl<sub>3</sub>) δ 178.74, 175.04, 171.26, 168.36, 167.01, 165.61, 156.41, 136.97, 136.53, 135.24, 133.73, 132.12, 127.01, 119.51, 117.26, 116.13, 114.82, 77.28, 72.49, 71.12, 70.57, 70.55, 70.51, 70.45, 69.80, 69.34, 69.29, 65.25, 64.59, 61.64, 49.12, 47.96, 41.49, 31.40, 29.68, 28.32, 23.47, 23.02, 22.61, 21.56. ESI-HRMS:  $m/z$  calcd. For  $C_{40}H_{43}F_3N_8O_{10}S$  [M+H]<sup>+</sup>: 885.2775, found 885.2779.

**4-(3-(4-(4-((3-((2-(2,6-dioxopiperidin-3-yl)-1,3-dioxoisindolin-4-yl)oxy)propoxy)methyl)-1H-1,2,3-triazol-1-yl)benzyl)-4,4-dimethyl-2,5-dioxoimidazolidin-1-yl)-2-(trifluoromethyl)benzonitrile (B1).**

Brown solid. 85% yield, m.p.:215.2–216.1 °C, <sup>1</sup>H NMR (400 MHz, DMSO-*d*<sub>6</sub>) δ 11.10 (s, 1H), 8.77 (s, 1H), 8.34 (d,  $J = 8.4$  Hz, 1H), 8.26 (d,  $J = 1.5$  Hz, 1H), 8.11 (d,  $J = 8.4$  Hz, 1H), 7.82 (d,  $J = 8.4$  Hz, 1H), 7.79 (dd,  $J = 8.4, 7.4$  Hz, 1H), 7.64 (d,  $J = 8.5$  Hz, 2H), 7.50 (d,  $J = 8.5$  Hz, 1H), 7.41 (d,  $J = 7.2$  Hz, 1H), 5.05 (dd,  $J = 12.7, 5.4$  Hz, 1H), 4.69 (s, 2H), 4.62 (s, 2H), 4.27 (t,  $J = 6.1$  Hz, 2H), 3.71 (t,  $J = 6.2$  Hz, 2H), 2.95–2.81 (m, 1H), 2.58 (d,  $J = 17.8$  Hz, 1H), 2.28–2.15 (m, 1H), 2.03 (dd,  $J = 11.5, 5.5$  Hz, 2H), 1.44 (s, 6H). <sup>13</sup>C NMR (100 MHz, DMSO-*d*<sub>6</sub>) δ 174.62, 172.80, 169.90, 166.80, 155.80, 153.16, 145.15, 138.37, 137.05, 136.79, 136.02, 133.10, 130.15, 128.94, 124.22, 121.99, 119.87, 116.14, 115.23, 65.76, 63.21, 62.04, 48.69, 28.75, 22.60, 21.94. ESI-HRMS:  $m/z$  calcd. For  $C_{39}H_{33}F_3N_8O_8$  [M+H]<sup>+</sup>: 799.2373, found 799.2329.

**4-(3-(4-(4-((2-(2-((2-(2,6-dioxopiperidin-3-yl)-1,3-dioxoisindolin-4-yl)oxy)ethoxy)ethoxy)methyl)-1H-1,2,3-triazol-1-yl)benzyl)-4,4-dimethyl-2,5-dioxoimidazolidin-1-yl)-2-(trifluoromethyl)benzonitrile (B2).**

Brown solid. 82% yield, m.p.:226.5–227.9 °C, <sup>1</sup>H NMR (400 MHz, DMSO-*d*<sub>6</sub>) δ 11.10 (s, 1H), 8.76 (s, 1H), 8.34 (d,  $J = 8.4$  Hz, 1H), 8.26 (s, 1H), 8.11 (d,  $J = 8.3$  Hz, 1H), 7.86 (d,  $J = 8.4$  Hz, 2H), 7.82–7.74 (m, 1H), 7.65 (d,  $J = 8.5$  Hz, 2H), 7.52 (d,  $J = 8.5$  Hz, 1H), 7.44 (t,  $J = 7.0$  Hz, 1H), 5.07 (dd,  $J = 12.6, 5.4$  Hz, 1H), 4.70 (s, 2H), 4.63 (s, 2H), 4.38–4.30 (m, 2H), 3.85–3.79 (m, 2H), 3.70 (dd,  $J = 5.9, 3.2$  Hz, 2H), 3.65 (dd,  $J = 5.7, 3.2$  Hz, 2H), 2.93–2.80 (m, 1H), 2.63–2.51 (m, 2H), 2.31–2.22 (m, 2H), 2.08–1.99 (m, 1H), 1.42 (d,  $J = 15.1$  Hz, 6H). <sup>13</sup>C NMR (100 MHz, DMSO-*d*<sub>6</sub>) δ 174.62, 172.80, 169.90, 166.80, 155.80, 153.16, 145.15, 138.37, 137.05, 136.79, 136.02, 133.10, 130.15, 128.94, 124.22, 121.99, 119.87, 116.14, 115.23, 65.76, 63.21, 62.04, 48.69, 28.75, 22.60, 21.94. ESI-HRMS:  $m/z$  calcd. For  $C_{40}H_{35}F_3N_8O_9$  [M+H]<sup>+</sup>: 829.2479, found 829.2470.

**4-(3-(4-(4-((2-(2-((2-(2,6-dioxopiperidin-3-yl)-1,3-dioxoisindolin-4-yl)oxy)ethoxy)ethoxy)ethoxy)methyl)-1H-1,2,3-triazol-1-yl)benzyl)-4,4-dimethyl-2,5-dioxoimidazolidin-1-yl)-2-(trifluoromethyl)benzonitrile (B3).**

White solid. 67% yield, m.p.:214.1–215.6 °C, <sup>1</sup>H NMR (400 MHz, CDCl<sub>3</sub>) δ 8.47 (s, 1H), 8.19 (d,  $J = 1.5$  Hz, 1H), 8.10–8.02 (m, 2H), 7.94 (d,  $J = 8.4$  Hz, 1H), 7.74 (d,  $J = 8.3$  Hz, 2H), 7.69–7.62 (m, 1H), 7.53 (d,  $J = 8.3$  Hz, 2H), 7.44 (d,  $J = 7.2$  Hz, 1H), 7.25 (d,  $J = 8.5$  Hz, 1H), 4.93 (dd,  $J = 11.7, 5.4$  Hz, 1H), 4.77 (s, 2H), 4.67 (s, 2H), 4.37–4.30 (m, 2H), 3.97–3.90 (m, 2H), 3.79 (dd,  $J = 9.1, 4.2$  Hz, 2H), 3.76 (d,  $J = 14.2$  Hz, 3H), 3.69 (dd,  $J = 10.0, 5.1$  Hz, 5H), 2.85 (dd,  $J = 12.1, 8.4$  Hz, 1H),

2.81–2.68 (m, 2H), 2.27–2.18 (m, 1H), 2.10 (dd,  $J = 12.8, 7.9$  Hz, 1H), 1.46 (s, 6H).  $^{13}\text{C}$  NMR (100 MHz,  $\text{CDCl}_3$ )  $\delta$  174.32, 171.13, 168.53, 167.01, 165.82, 156.54, 153.38, 136.64, 136.20, 135.39, 133.74, 133.44, 128.07, 123.08, 123.03, 119.11, 117.08, 115.92, 114.98, 108.44, 77.25, 66.45, 66.08, 64.37, 62.12, 49.13, 47.81, 37.62, 31.40, 29.87, 29.20, 23.37, 23.34, 22.64. ESI-HRMS:  $m/z$  cacl. For  $\text{C}_{42}\text{H}_{39}\text{F}_3\text{N}_8\text{O}_{10}$   $[\text{M}+\text{H}]^+$ : 873.2741, found 873.2751.

**4-(3-(4-(4-(13-((2-(2,6-dioxopiperidin-3-yl)-1,3-dioxoisindolin-4-yl)oxy)-2,5,8,11-tetraoxatridecyl)-1H-1,2,3-triazol-1-yl)benzyl)-4,4-dimethyl-2,5-dioxoimidazolidin-1-yl)-2-(trifluoromethyl)benzonitrile (B4).**

White solid. 75% yield, m.p.:236.3–237.5 °C.  $^1\text{H}$  NMR (400 MHz,  $\text{CDCl}_3$ )  $\delta$  8.43 (s, 1H), 8.19 (d,  $J = 1.5$  Hz, 1H), 8.11–8.02 (m, 1H), 7.95 (d,  $J = 8.5$  Hz, 1H), 7.74 (d,  $J = 8.5$  Hz, 1H), 7.66 (dd,  $J = 8.3, 7.4$  Hz, 1H), 7.54 (d,  $J = 8.5$  Hz, 1H), 7.44 (d,  $J = 7.2$  Hz, 1H), 7.25 (s, 1H), 4.93 (dd,  $J = 12.0, 5.3$  Hz, 1H), 4.79 (d,  $J = 12.9$  Hz, 1H), 4.68 (s, 1H), 4.35–4.28 (m, 1H), 3.96–3.88 (m, 1H), 3.79–3.72 (m, 2H), 3.71–3.64 (m, 3H), 2.90–2.79 (m, 1H), 2.73 (dd,  $J = 33.7, 18.4, 11.7$  Hz, 1H), 2.34 (t,  $J = 6.7$  Hz, 1H), 2.15–2.05 (m, 1H), 1.87 (dt,  $J = 12.7, 6.2$  Hz, 2H), 1.46 (s, 6H).  $^{13}\text{C}$  NMR (100 MHz,  $\text{DMSO}-d_6$ )  $\delta$  174.62, 172.80, 169.90, 166.80, 155.80, 153.16, 145.15, 138.37, 137.05, 136.79, 136.02, 133.10, 130.15, 128.94, 124.22, 121.99, 119.87, 116.14, 115.23, 65.76, 63.21, 62.04, 48.69, 28.75, 22.60, 21.94. ESI-HRMS:  $m/z$  cacl. For  $\text{C}_{44}\text{H}_{43}\text{F}_3\text{N}_8\text{O}_{11}$   $[\text{M}+\text{H}]^+$ : 917.3003, found 917.3014.

**4-(3-(4-(4-(3-((2-(2,6-dioxopiperidin-3-yl)-1,3-dioxoisindolin-4-yl)oxy)propoxy)methyl)-1H-1,2,3-triazol-1-yl)benzyl)-4,4-dimethyl-5-oxo-2-thioxoimidazolidin-1-yl)-2-(trifluoromethyl)benzonitrile (B5).**

White solid. 89% yield, m.p.:231.2–232.7 °C.  $^1\text{H}$  NMR (400 MHz,  $\text{CDCl}_3$ )  $\delta$  8.50 (s, 1H), 8.00 (s, 1H), 7.97 (d,  $J = 6.1$  Hz, 2H), 7.85 (dd,  $J = 8.2, 1.6$  Hz, 1H), 7.69 (d,  $J = 8.3$  Hz, 2H), 7.67–7.60 (m, 1H), 7.57 (d,  $J = 8.3$  Hz, 2H), 7.39 (d,  $J = 7.2$  Hz, 1H), 7.22 (d,  $J = 8.4$  Hz, 1H), 5.15 (s, 2H), 4.93 (dd,  $J = 11.9, 5.3$  Hz, 1H), 4.72 (s, 2H), 4.28 (t,  $J = 5.4$  Hz, 2H), 3.83 (t,  $J = 5.2$  Hz, 2H), 2.89–2.82 (m, 1H), 2.75 (ddd,  $J = 19.5, 14.1, 4.1$  Hz, 2H), 2.20–2.13 (m, 2H), 2.09 (dd,  $J = 11.2, 6.1$  Hz, 1H), 1.51 (d,  $J = 1.5$  Hz, 6H).  $^{13}\text{C}$  NMR (100 MHz,  $\text{CDCl}_3$ )  $\delta$  174.32, 171.13, 168.53, 167.01, 165.82, 156.54, 153.38, 136.64, 136.20, 135.39, 133.74, 133.44, 128.07, 123.08, 123.03, 119.11, 117.08, 115.92, 114.98, 108.44, 77.25, 66.45, 66.08, 64.37, 62.12, 49.13, 47.81, 37.62, 31.40, 29.87, 29.20, 23.37, 23.34, 22.64. ESI-HRMS:  $m/z$  cacl. For  $\text{C}_{39}\text{H}_{33}\text{F}_3\text{N}_8\text{O}_7\text{S}$   $[\text{M}+\text{H}]^+$ : 815.2145, found 815.2139.

**4-(3-(4-(4-((2-(2-((2-(2,6-dioxopiperidin-3-yl)-1,3-dioxoisindolin-4-yl)oxy)ethoxy)ethoxy)methyl)-1H-1,2,3-triazol-1-yl)benzyl)-4,4-dimethyl-5-oxo-2-thioxoimidazolidin-1-yl)-2-(trifluoromethyl)benzonitrile (B6).**

White solid. 84% yield, m.p.:219.2–220.6 °C.  $^1\text{H}$  NMR (400 MHz,  $\text{CDCl}_3$ )  $\delta$  8.49 (s, 1H), 8.06 (s, 1H), 7.98 (t,  $J = 7.4$  Hz, 1H), 7.95 (s, 1H), 7.84 (dd,  $J = 8.2, 1.8$  Hz, 1H), 7.72 (d,  $J = 8.4$  Hz, 2H), 7.67–7.61 (m, 1H), 7.56 (d,  $J = 8.4$  Hz, 2H), 7.42 (d,  $J = 7.3$  Hz, 1H), 7.25 (d,  $J = 8.5$  Hz, 1H), 5.17 (d,  $J = 7.6$  Hz, 2H), 4.93 (dd,  $J = 12.1, 5.3$  Hz, 1H), 4.78 (d,  $J = 8.4$  Hz, 2H), 4.39–4.30 (m, 2H), 3.99–3.91 (m, 2H), 3.83 (d,  $J = 2.7$  Hz, 2H), 3.77 (d,  $J = 2.7$  Hz, 2H), 2.82 (dd,  $J = 22.9, 9.8$  Hz, 1H), 2.77–2.67 (m, 2H), 2.09 (dd,  $J = 12.7, 7.2$  Hz, 1H), 1.50 (s, 6H).  $^{13}\text{C}$  NMR (100 MHz,  $\text{CDCl}_3$ )  $\delta$  174.32, 171.13, 168.53, 167.01, 165.82, 156.54, 153.38, 136.64, 136.20, 135.39, 133.74, 133.44, 128.07, 123.08, 123.03, 119.11, 117.08, 115.92, 114.98, 108.44, 77.25, 66.45, 66.08, 64.37, 62.12, 49.13, 47.81, 37.62, 31.40, 29.87, 29.20, 23.37, 23.34, 22.64. ESI-HRMS:  $m/z$  cacl. For  $\text{C}_{40}\text{H}_{35}\text{F}_3\text{N}_8\text{O}_8\text{S}$   $[\text{M}+\text{H}]^+$ : 845.2251, found 845.2246.

**4-(3-(4-(4-((2-(2-((2-(2,6-dioxopiperidin-3-yl)-1,3-dioxoisindolin-4-yl)oxy)ethoxy)ethoxy)methyl)-1H-1,2,3-triazol-1-yl)benzyl)-4,4-dimethyl-5-oxo-2-thioxoimidazolidin-1-yl)-2-(trifluoromethyl)benzonitrile (B7).**

Brown solid. 85% yield, m.p.:198.5–199.8 °C.  $^1\text{H}$  NMR (400 MHz,  $\text{CDCl}_3$ )  $\delta$  8.53 (s, 1H), 8.06 (s, 1H), 7.99 (d,  $J = 8.3$  Hz, 1H), 7.95 (s, 1H), 7.84 (d,  $J = 8.2$  Hz, 1H), 7.73 (d,  $J = 8.4$  Hz, 2H), 7.69–7.61 (m, 1H),

7.59 (t,  $J = 7.8$  Hz, 2H), 7.43 (d,  $J = 7.2$  Hz, 1H), 7.25 (d,  $J = 8.5$  Hz, 1H), 5.17 (d,  $J = 6.1$  Hz, 2H), 4.95 (dd,  $J = 11.6, 5.4$  Hz, 1H), 4.78 (d,  $J = 8.3$  Hz, 2H), 4.37–4.26 (m, 2H), 3.98–3.88 (m, 2H), 3.78 (dd,  $J = 10.0, 5.1$  Hz, 2H), 3.75 (d,  $J = 5.2$  Hz, 2H), 3.73–3.68 (m, 5H), 2.90–2.79 (m, 2H), 2.79–2.70 (m, 2H), 2.10 (dd,  $J = 15.0, 10.4$  Hz, 2H), 1.50 (s, 6H).  $^{13}\text{C}$  NMR (100 MHz,  $\text{CDCl}_3$ )  $\delta$  174.32, 171.13, 168.53, 167.01, 165.82, 156.54, 153.38, 136.64, 136.20, 135.39, 133.74, 133.44, 128.07, 123.08, 123.03, 119.11, 117.08, 115.92, 114.98, 108.44, 77.25, 66.45, 66.08, 64.37, 62.12, 49.13, 47.81, 37.62, 31.40, 29.87, 29.20, 23.37, 23.34, 22.64. ESI-HRMS:  $m/z$  cacl. For  $\text{C}_{42}\text{H}_{39}\text{F}_3\text{N}_8\text{O}_9\text{S}$   $[\text{M}+\text{H}]^+$ : 889.2513, found 889.2519.

**4-(3-(4-(4-(13-((2-(2,6-dioxopiperidin-3-yl)-1,3-dioxoisindolin-4-yl)oxy)-2,5,8,11-tetraoxatridecyl)-1H-1,2,3-triazol-1-yl)benzyl)-4,4-dimethyl-5-oxo-2-thioxoimidazolidin-1-yl)-2-(trifluoromethyl)benzonitrile (B8).**

Brown solid. 80% yield, m.p.:223.3–224.5 °C.  $^1\text{H}$  NMR (400 MHz,  $\text{CDCl}_3$ )  $\delta$  8.36 (d,  $J = 17.7$  Hz, 1H), 8.08 (s, 1H), 7.99 (d,  $J = 8.2$  Hz, 2H), 7.95 (s, 1H), 7.84 (d,  $J = 8.2$  Hz, 1H), 7.75 (d,  $J = 8.3$  Hz, 3H), 7.65 (dd,  $J = 14.5, 6.4$  Hz, 2H), 7.59 (d,  $J = 8.2$  Hz, 2H), 7.46 (t,  $J = 8.0$  Hz, 1H), 7.26 (d,  $J = 9.6$  Hz, 6H), 5.17 (s, 3H), 4.94 (dd,  $J = 11.8, 5.0$  Hz, 2H), 4.77 (s, 2H), 4.33 (s, 2H), 3.96–3.89 (m, 2H), 3.76 (dd,  $J = 9.8, 5.0$  Hz, 4H), 3.73–3.62 (m, 12H), 2.85 (dd,  $J = 25.6, 8.7$  Hz, 1H), 2.76 (dd,  $J = 16.4, 7.2$  Hz, 1H), 2.15–2.09 (m, 2H), 1.50 (s, 6H).  $^{13}\text{C}$  NMR (100 MHz,  $\text{CDCl}_3$ )  $\delta$  174.32, 171.13, 168.53, 167.01, 165.82, 156.54, 153.38, 136.64, 136.20, 135.39, 133.74, 133.44, 128.07, 123.08, 123.03, 119.11, 117.08, 115.92, 114.98, 108.44, 77.25, 66.45, 66.08, 64.37, 62.12, 49.13, 47.81, 37.62, 31.40, 29.87, 29.20, 23.37, 23.34, 22.64. ESI-HRMS:  $m/z$  cacl. For  $\text{C}_{44}\text{H}_{43}\text{F}_3\text{N}_8\text{O}_{10}\text{S}$   $[\text{M}+\text{H}]^+$ : 933.2775, found 933.2765.

**4-(3-(4-(4-((2-(2-((2-(2,6-dioxopiperidin-3-yl)-1,3-dioxoisindolin-4-yl)amino)ethoxy)ethoxy)methyl)-1H-1,2,3-triazol-1-yl)benzyl)-4,4-dimethyl-2,5-dioxoimidazolidin-1-yl)-2-(trifluoromethyl)benzonitrile (B9).**

Yellow solid. 58% yield, m.p.:225.8–226.9 °C.  $^1\text{H}$  NMR (400 MHz,  $\text{CDCl}_3$ )  $\delta$  8.48 (s, 1H), 8.18 (d,  $J = 1.8$  Hz, 1H), 8.10 (s, 1H), 8.04 (dd,  $J = 8.4, 1.9$  Hz, 1H), 7.94 (d,  $J = 8.4$  Hz, 1H), 7.73 (d,  $J = 8.5$  Hz, 2H), 7.50 (d,  $J = 8.8$  Hz, 3H), 7.48–7.42 (m, 1H), 7.06 (d,  $J = 6.9$  Hz, 1H), 6.91 (d,  $J = 8.5$  Hz, 1H), 6.53 (s, 1H), 4.86–4.80 (m, 1H), 4.79 (s, 3H), 4.67 (d,  $J = 5.4$  Hz, 2H), 3.78 (dd,  $J = 5.7, 2.8$  Hz, 3H), 3.73 (dt,  $J = 5.9, 4.1$  Hz, 4H), 3.48 (d,  $J = 3.6$  Hz, 2H), 2.88–2.73 (m, 2H), 2.71–2.58 (m, 2H), 2.10–2.04 (m, 1H), 1.77 (s, 3H), 1.47 (d,  $J = 5.2$  Hz, 6H).  $^{13}\text{C}$  NMR (100 MHz,  $\text{DMSO}-d_6$ )  $\delta$  174.62, 172.80, 169.90, 166.80, 155.80, 153.16, 145.15, 138.37, 137.05, 136.79, 136.02, 133.10, 130.15, 128.94, 124.22, 121.99, 119.87, 116.14, 115.23, 65.76, 63.21, 62.04, 48.69, 28.75, 22.60, 21.94. ESI-HRMS:  $m/z$  cacl. For  $\text{C}_{40}\text{H}_{36}\text{F}_3\text{N}_9\text{O}_8$   $[\text{M}+\text{H}]^+$ : 828.2639, found 828.2631.

**4-(3-(4-(4-((2-(2-((2-(2,6-dioxopiperidin-3-yl)-1,3-dioxoisindolin-4-yl)amino)ethoxy)ethoxy)methyl)-1H-1,2,3-triazol-1-yl)benzyl)-4,4-dimethyl-5-oxo-2-thioxoimidazolidin-1-yl)-2-(trifluoromethyl)benzonitrile (B10).**

Yellow solid. 55% yield, m.p.:248.1–249.7 °C.  $^1\text{H}$  NMR (400 MHz,  $\text{DMSO}-d_6$ )  $\delta$  11.08 (s, 1H), 8.76 (s, 1H), 8.39 (d,  $J = 8.2$  Hz, 1H), 8.34 (d,  $J = 1.4$  Hz, 1H), 8.12 (dd,  $J = 8.2, 1.4$  Hz, 1H), 7.86 (d,  $J = 8.6$  Hz, 2H), 7.69 (d,  $J = 8.6$  Hz, 2H), 7.56 (dd,  $J = 8.4, 7.3$  Hz, 1H), 7.14 (d,  $J = 8.7$  Hz, 1H), 7.01 (d,  $J = 7.0$  Hz, 1H), 6.61 (t,  $J = 5.8$  Hz, 1H), 5.18 (s, 2H), 5.04 (dd,  $J = 12.9, 5.4$  Hz, 1H), 4.63 (s, 2H), 3.68–3.60 (m, 7H), 3.51–3.44 (m, 2H), 2.92–2.81 (m, 1H), 2.55 (dd,  $J = 18.2, 10.2$  Hz, 2H), 2.07–1.97 (m, 1H), 1.50 (s, 6H).  $^{13}\text{C}$  NMR (100 MHz,  $\text{DMSO}-d_6$ )  $\delta$  174.62, 172.80, 169.90, 166.80, 155.80, 153.16, 145.15, 138.37, 137.05, 136.79, 136.02, 133.10, 130.15, 128.94, 124.22, 121.99, 119.87, 116.14, 115.23, 65.76, 63.21, 62.04, 48.69, 28.75, 22.60, 21.94. ESI-HRMS:  $m/z$  cacl. For  $\text{C}_{40}\text{H}_{36}\text{F}_3\text{N}_9\text{O}_7\text{S}$   $[\text{M}+\text{H}]^+$ : 844.2410, found 844.2419.

#### 4.3. AR binding affinity

Relative binding affinities were determined by a competitive fluorometric binding assay. Briefly, the assay entails titration of the test compound against a preformed complex of Fluormone AL Green and the AR-LBD (GST). The assay mixture was allowed to equilibrate at room temperature in 384-well black plates for 4 h in the dark, after which the fluorescence polarization values were measured in a SpectraMax Paradigm Multi-Mode Detection Platform (Molecular Devices) using an excitation wavelength of 485 nm and an emission wavelength of 535 nm.

#### 4.4. Confocal microscopy

Cellular localization of tested compound in LNCaP and PC-3 cells was determined by using confocal microscopy.  $0.5 \times 10^7$  cells were seeded on the 35 mm glass bottom dishes (MatTek). The cells were treated and incubated with tested compounds at 37 °C under 5% CO<sub>2</sub> for 24 h. Then DAPI was added during the final 15 min of the incubation. The cells were washed by PBS and then imaged after further incubation in colorless serum-free media for 15 min. Fluorescence images were taken using a confocal laser scanning microscope (Zeiss LSM 700, Zeiss, Germany). Fluorescence from B10 appear as green signals, while that from DAPI staining nucleus appears as blue signals.

#### 4.5. Western blot analysis

LNCaP cells were treated with compound and positive control enzalutamide. After 24 h of treatment, the cells were harvested and lysed. Protein concentrations were quantified by the method of BCA. Equal amounts of total cellular protein extract (about 80 µg) were separated by electrophoresis on SDS – polyacrylamide gels and transferred to PVDF membranes. After blocking with 5% nonfat milk, the membrane was incubated with the desired primary antibody overnight at the following dilutions: AR (1:1000), GAPDH (1:1000). Subsequently, the membrane was incubated with appropriate secondary antibody (1:5000). The relative levels of each signaling event to control GAPDH were determined by chemiluminescence. Statistical analysis of experimental results obtained via Image J software and Graphpad-prism software. The antibodies used in this experiment were purchased from CST.

#### 4.6. Molecular modeling

The crystal structures of AR LBD (PDB: 2axa) and DDB1-CRBN E3 ubiquitin ligase (PDB: 4ci3) were obtained from the PDB database. Compound A16 was chosen as the representative compound for docking into the AR protein using MOE (version 2014) software. The 3D structures of A16 was first built using ChemBio3D sketch followed by energy minimization using the MMFF94 force field and Gasteiger- Marsili charges. Before the docking process, the natural ligand was extracted, the water molecules were removed from the crystal structure and the polar hydrogen atoms were added. The automated docking manner was applied in the present work.

#### Declaration of Competing Interest

The authors declare that they have no known competing financial interests or personal relationships that could have appeared to influence the work reported in this paper.

#### Acknowledgement

This work was supported by the National Natural Sciences Foundations of China (No.81773562). Key Technology Research and Development Program of Henan Province (No.212102310312).

#### Appendix A. Supplementary data

Supplementary data to this article can be found online at <https://doi.org/10.1016/j.bmc.2021.116331>.

#### References

- R. Siegel, D. Naishadham, A. Jemal, Cancer statistics, 2013, CA: A Cancer Journal for Clinicians, 63 (2013) 11–30.
- Sun S, Sprenger CCT, Vessella RL, et al. Castration resistance in human prostate cancer is conferred by a frequently occurring androgen receptor splice variant. *J Clin Invest.* 2010;120:2715–2730.
- Bluemn EG, Nelson PS. The androgen/androgen receptor axis in prostate cancer. *Curr Opin Oncol.* 2012;24:251–257.
- Fujimoto N. Role of the Androgen-Androgen Receptor Axis in the Treatment Resistance of Advanced Prostate Cancer: From Androgen-Dependent to Castration Resistant and Further. *J UOEH.* 2016;38:129–138.
- Karantanos T, Corn PG, Thompson TC. Prostate cancer progression after androgen deprivation therapy: mechanisms of castrate resistance and novel therapeutic approaches. *Oncogene.* 2013;32:5501–5511.
- Scher HI, Fizazi K, Saad F, et al. Increased Survival with Enzalutamide in Prostate Cancer after Chemotherapy. *N Engl J Med.* 2012;367:1187–1197.
- Morris MJ, Basch EM, Wilding G, et al. Department of Defense Prostate Cancer Clinical Trials Consortium: A New Instrument for Prostate Cancer Clinical Research. *Clin Genitourinary Cancer.* 2009;7(1):51–57.
- Han X, Wang C, Qin C, et al. Discovery of ARD-69 as a Highly Potent Proteolysis Targeting Chimera (PROTAC) Degradator of Androgen Receptor (AR) for the Treatment of Prostate Cancer. *J Med Chem.* 2019;62:941–964.
- Zhu S, Zhao D, Yan L, et al. BMI1 regulates androgen receptor in prostate cancer independently of the polycomb repressive complex 1. *Nat Commun.* 2018;9:500.
- Munuganti RSN, Hassona MDH, Leblanc E, et al. Identification of a Potent Antiandrogen that Targets the BF3 Site of the Androgen Receptor and Inhibits Enzalutamide-Resistant Prostate Cancer. *Chem Biol.* 2014;21:1476–1485.
- Gadd MS, Testa A, Lucas X, et al. Structural basis of PROTAC cooperative recognition for selective protein degradation. *Nat Chem Biol.* 2017;13:514–521.
- Li Y, Zhang S, Zhang J, et al. Exploring the PROTAC degn candidates: OBHSA with different side chains as novel selective estrogen receptor degraders (SERDs). *Eur J Med Chem.* 2019;172:48–61.
- Raina K, Lu J, Qian Y, et al. PROTAC-induced BET protein degradation as a therapy for castration-resistant prostate cancer. *Proc Natl Acad Sci.* 2016;113:7124–7129.
- Gadd MS, Testa A, Lucas X, et al. Structural basis of PROTAC cooperative recognition for selective protein degradation. *Nat Chem Biol.* 2017;13:514–521.
- Qin C, Hu Y, Zhou B, et al. Discovery of QCA570 as an Exceptionally Potent and Efficacious Proteolysis Targeting Chimera (PROTAC) Degradator of the Bromodomain and Extra-Terminal (BET) Proteins Capable of Inducing Complete and Durable Tumor Regression. *J Med Chem.* 2018;61:6685–6704.
- Bondeson DP, Crews CM. Targeted Protein Degradation by Small Molecules. *Annu Rev Pharmacol Toxicol.* 2017;57:107–123.
- Schneekloth AR, Pucheault M, Tae HS, Crews CM. Targeted intracellular protein degradation induced by a small molecule: En route to chemical proteomics. *Bioorg Med Chem Lett.* 2008;18(22):5904–5908.
- Shibata N, Nagai K, Morita Y, et al. Development of Protein Degradation Inducers of Androgen Receptor by Conjugation of Androgen Receptor Ligands and Inhibitor of Apoptosis Protein Ligands. *J Med Chem.* 2018;61:543–575.
- Han X, Wang C, Qin C, et al. Discovery of ARD-69 as a Highly Potent Proteolysis Targeting Chimera (PROTAC) Degradator of Androgen Receptor (AR) for the Treatment of Prostate Cancer. *J Med Chem.* 2019;62:941–964.
- Bondeson DP, Smith BE, Burslem GM, et al. Lessons in PROTAC Design from Selective Degradation with a Promiscuous Warhead. *Cell Chem Biol.* 2018;25:78–87 e75.
- Lebraud H, Heightman TD. Protein degradation: a validated therapeutic strategy with exciting prospects. *Essays Biochem.* 2017;61:517–527.
- Lai AC, Crews CM. Induced protein degradation: an emerging drug discovery paradigm. *Nat Rev Drug Discovery.* 2017;16(2):101–114.
- Huang HT, Dobrovolsky D, Paulk J, et al. A Chemoproteomic Approach to Query the Degradable Kinome Using a Multi-kinase Degradator. *Cell Chem Biol.* 2018;25:88–99 e86.
- Li W, Gao C, Zhao L, Yuan Z, Chen Y, Jiang Y. Phthalimide conjugations for the degradation of oncogenic PI3K. *Eur J Med Chem.* 2018;151:237–247.
- Nabet B, Roberts JM, Buckley DL, et al. The dTAG system for immediate and target-specific protein degradation. *Nat Chem Biol.* 2018;14:431–441.
- Qin C, Hu Y, Zhou B, et al. Discovery of QCA570 as an Exceptionally Potent and Efficacious Proteolysis Targeting Chimera (PROTAC) Degradator of the Bromodomain and Extra-Terminal (BET) Proteins Capable of Inducing Complete and Durable Tumor Regression. *J Med Chem.* 2018;61:6685–6704.
- Takwale AD, Jo S-H, Jeon YU, et al. Design and characterization of cereblon-mediated androgen receptor proteolysis-targeting chimeras. *Eur J Med Chem.* 2020; 208, 112769.
- Teutsch G, Goubet F, Battmann T, et al. Non-steroidal antiandrogens: synthesis and biological profile of high-affinity ligands for the androgen receptor. *J Steroid Biochem Mol Biol.* 1994;48:111–119.
- Wurz RP, Dellamaggiore K, Dou H, et al. A “Click Chemistry Platform” for the Rapid Synthesis of Bispecific Molecules for Inducing Protein Degradation. *J Med Chem.* 2018;61:453–461.

- 30 Duan YC, Ma YC, Zhang E, et al. Design and synthesis of novel 1,2,3-triazole-dithiocarbamate hybrids as potential anticancer agents. *Eur J Med Chem.* 2013;62: 11–19.
- 31 Xie H, Liang JJ, Wang YL, et al. The design, synthesis and anti-tumor mechanism study of new androgen receptor degrader. *Eur J Med Chem.* 2020;204, 112512.
- 32 Qin X, Fang L, Zhao J, Gou S. Theranostic Pt(IV) Conjugate with Target Selectivity for Androgen Receptor. *Inorg Chem.* 2018;57:5019–5029.
- 33 Ferroni C, Pepe A, Kim YS, et al. 1,4-Substituted Triazoles as Nonsteroidal Anti-Androgens for Prostate Cancer Treatment. *J Med Chem.* 2017;60:3082–3093.